

Supporting Information for:

Synthesis and Photophysics Properties of Ruthenium (II) Polyimine Complexes Decorated with Flavin

Huimin Guo[†],^{} Lijuan Zhu[†], Can Dang[†], Jianzhang Zhao[†],^{*}, Bernhard Dick[‡]*

[†] State Key Laboratory of Fine Chemicals, School of Chemistry, Dalian University of Technology, Dalian, 116024, P. R. China.

[‡] Institut für Physikalische und Theoretische Chemie, Universität Regensburg, Regensburg, 93053, Germany

Contents

1. General Information.....	Page 2
2. Synthesis and Molecular Structure Characterization Data.....	Page 4
3. NMR and HRMS spectra.....	Page 12
4. TD-DFT Calculations and NTO Analysis.....	Page 27

^{*} Corresponding authors, email: guohm@dlut.edu.cn(H. G.); zhaojzh@dlut.edu.cn (J. Z.).

1. General Information

All the chemicals used in synthesis are analytical pure and were used as received. Solvents were dried and distilled before used for synthesis. All samples in flash photolysis and upconversion experiments were deaerated with N₂ for 15 min before measurement.

Analytical Measurements. All chemicals are analytically pure and used as received. NMR spectra were recorded by Bruker 500 MHz spectrometer and OXFPRD NMR 400 MHz spectrometer with CDCl₃, DMSO-d₆ or Acetonitrile-d₆ as solvents and tetramethylsilane (TMS) as standard at 0.00 ppm. HRMS was accomplished with MALDI micro MX (Waters, U.S.), GCT (Micromass, U.K.), G6224A (Aglient, U.S.) or LTQ Orbitrap XL (Thermo Scientific, U.S.). Fluorescence spectra were measured on an RF5301 PC spectrofluorometer (Shimadzu, Japan). Absorption spectra were recorded on UV2550 UV–Vis spectrophotometer (Shimadzu, Japan). Fluorescence lifetimes were measured with an OB920 luminescence lifetime spectrometer (Edinburgh, UK).

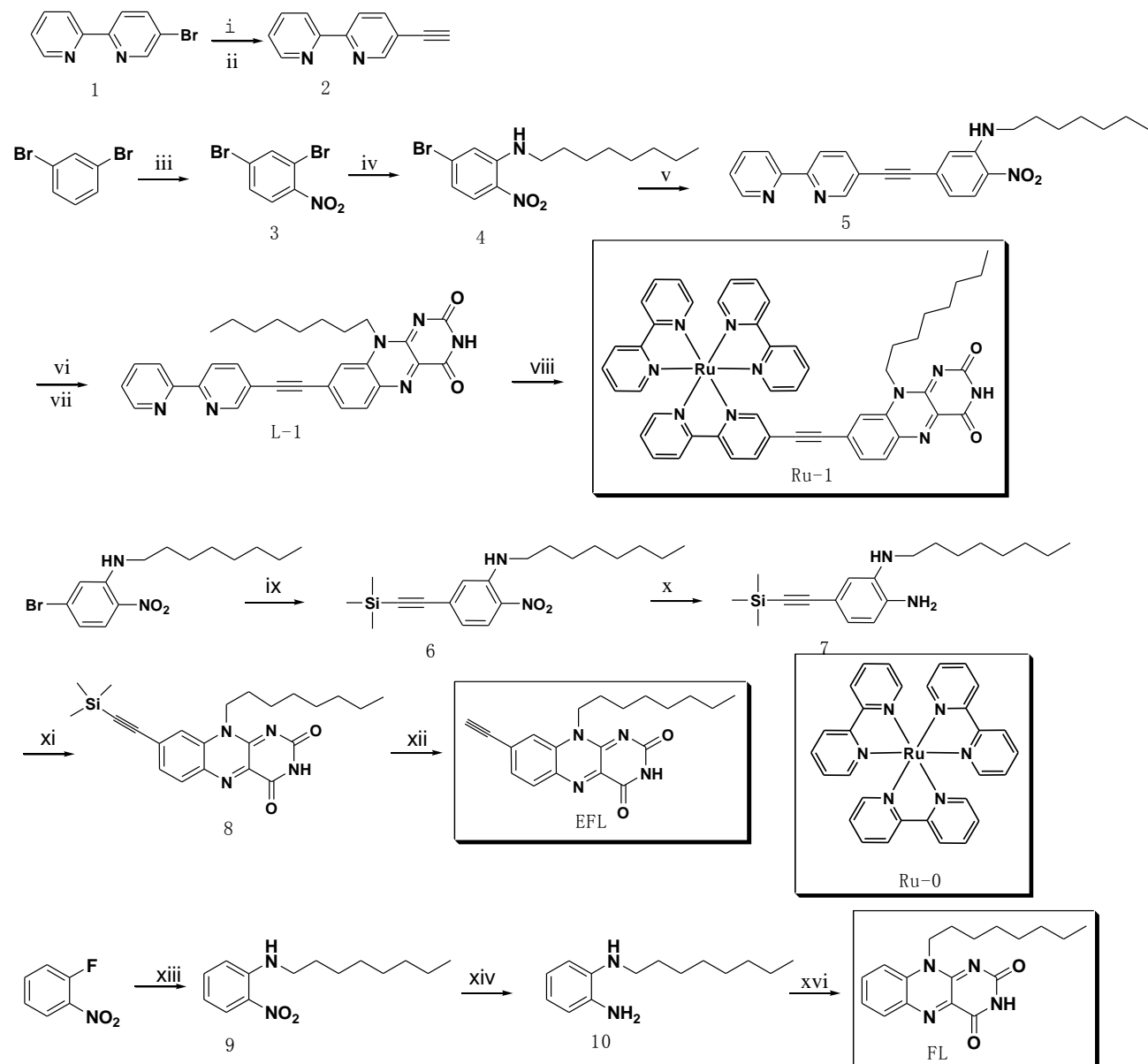
Nanosecond Transient Absorption Spectra. The nanosecond transient absorption spectra were measured on LP980 laser flash photolysis spectrometer (Edinburgh Instruments, UK) and recorded on a Tektronix TDS 3012B oscilloscope and with a nanosecond pulsed laser (OpoletteTM 355II+UV nanosecond pulsed laser, typical pulse length: 7 ns. Pulse repetition: 20 Hz. Peak OPO energy: 6 mJ. The wavelength is tunable in the range of 200–2200 nm. OPOTEK, USA). The lifetime values (by monitoring the decay trace of the transients) were obtained with the LP900 software.

Cyclic Voltammetry. Cyclic voltammetry was performed under a 50 mV/s scan rate, in CHI610D Electrochemical workstation (Shanghai, China). The measurements were performed at room temperature with tetrabutylammonium hexafluorophosphate (Bu₄N[PF₆], 0.1 M) as the supporting electrolyte, glassy carbon electrode as the working electrode, and platinum electrode as the counter electrode. Acetonitrile was used as the solvent, and ferrocene (Fc) was added as the internal reference. The solution was purged with N₂ before measurement, and the N₂ gas flow was kept constant during the measurement.

Triplet-Triplet Annihilation Upconversion. 473 nm cw-laser was used for the upconversion. The upconversion quantum yield (Φ_{UC}) was determined with prompt fluorescence of $\text{Ru}(\text{bpy})_3^{2+}$ ($\Phi_F = 9.5\%$ in MeCN) as the standard. The upconversion quantum yield was calculated with following Eq. S1, where F_{UC} , A_{sam} , I_{sam} , and η_{sam} represents the quantum yield, absorbance, integrated photoluminescence intensity, and refractive index of the sample. The corresponding terms for the subscript std are for the reference quantum counter. The equation is multiplied by a factor of 2 so as to set the maximum quantum yield to unity.

$$\Phi_{\text{UC}} = 2 \Phi_{\text{std}} \left(\frac{1 - 10^{-A_{\text{sam}}}}{1 - 10^{-A_{\text{std}}}} \right) \left(\frac{I_{\text{sam}}}{I_{\text{std}}} \right) \left(\frac{\eta_{\text{sam}}}{\eta_{\text{std}}} \right)^2 \quad (\text{eq. 1})$$

2. Synthesis and Molecular Structure Characterization Data



Scheme S1. Synthesis of the compounds. (i) Trimethylsilylacetylene, $\text{Pd}(\text{PPh}_3)_2\text{Cl}_2$, PPh_3 , CuI , Et_3N , reflux, 8h. Yield=66.2%; (ii) Bu_4NF , THF, r.t. Yield=58.2%; (iii) Concentrated sulphuric acid, concentrated nitric acid, r.t, 2h. Yield=73.8%; (iv) N-octylamine, Et_3N , THF, reflux, 15h. Yield=98.7%; (v) $\text{Pd}(\text{PPh}_3)_4$, CuI , Et_3N , reflux, 8h. Yield=71%; (vi) Zinc, ammonium chloride,

methanol, H₂O, reflux. 3h; (vii) Alloxan, boric acid, acetic acid glacial, 60°C, 1h. Yield=33.7%; (viii) [RuCl₂(cymene)]₂, 2,2'-Dipyridyl, ethanol, H₂O. Yield=15%; (ix) Trimethylsilylacetylene, Pd(PPh₃)₄, CuI, Et₃N, reflux, 8h. Yield=52%; (x) Zinc, ammonium chloride, methanol, H₂O. Yield=82%; (xi) Alloxan, boric acid, acetic acid glacial, 60°C, 1h. Yield=69.8%; (xii) Bu₄NF, THF, 0°C, 1h. Yield=71.4%; (xiii) N-octylamine, Et₃N, THF, reflux, 9h. Yield=98.5%; (xiv) Zinc, ammonium chloride, methanol, H₂O. Yield=95%; (xvi) Alloxan, boric acid, acetic acid glacial, 60°C, 1h. Yield=41%.

Synthesis of compound 3: 1, 3-Dibromobenzene (472mg, 2 mmol) was added to an ice-cooled mixture of concentrated sulfuric acid (1 mL) and concentrated nitric acid (1 mL) at such a rate that the temperature was kept at 20°C. The reaction mixture was effectively stirred at room temperature for 4 hours and then cooled at 0 °C while ice (25 g) was added in small portions. The yellow precipitate was filtered off, washed with water and dried under vacuum. Then the solid was dissolve in CH₂Cl₂ and purified using column chromatography (silica gel, CH₂Cl₂: Petroleum ether = 1 : 2, v/v) to give a pale yellow solid(415.4mg, yield=73.8%). ¹H NMR (400 MHz, CDCl₃): δ 7.93 (s, 1H), 7.76(d, 1H, J=8.0Hz), 7.60(m, 1H). EI-TOF-HRMS ([C₆H₃NO₂Br₂+2H]⁺): calcd. 280.8510; found 280.8480.

Synthesis of compound 4: To a solution of 3 (213.5mg, 0.76 mmol) in THF (50 mL) was added n-octylamine (0.8 mL, 3.99 mmol) and triethylamine (0.2 mL). The solution was stirred under reflux for 15 hours. The solution was concentrated in vacuum and purified using column chromatography (silica gel, CH₂Cl₂ : Petroleum ether = 1: 3, v/v) to yield bright orange solid (247.5mg, 98.7%). ¹H NMR (400MHz,CDCl₃):δ 8.02 (d, 2H, J=12Hz), 7.01 (s, 1H), 6.74 (m, 1H), 3.26 (m, 2H), 1.73

(m, 2H), 1.48-1.41 (m, 2H), 1.37-1.24 (m, 8H), 0.89 (m, 3H). ^{13}C NMR (125 MHz. CDCl_3): 145.84, 131.62, 130.70, 128.09, 118.37, 116.36, 43.15, 31.71, 29.16, 29.10, 28.75, 26.97, 22.59, 14.03. ESI-TOF-HRMS $[(\text{C}_{14}\text{H}_{21}\text{BrN}_2\text{O}_2+\text{H})^+]$: calcd. 329.0864; found 329.0870.

Synthesis of compound 5: 4 (206mg, 0.63 mmol) and 2(170mg, 0.94mmol) was dissolved in 25 mL of Et_3N was added under N_2 . $\text{Pd}(\text{PPh}_3)_4$ (30 mg, 0.03 mmol) were added, followed by CuI (15mg, 0.05 mmol). The mixture was stirred under N_2 for 8h at 89 °C. After the reaction was finished, the solvent was removed under reduced pressure. The residue was purified by column chromatography (silica gel, CH_2Cl_2 : ethyl acetate = 1: 1, v/v). 4 was collected as an orange solid (187.3 mg, yield: 71.0%). ^1H NMR (400MHz, CDCl_3): δ 8.86 (s,1H), 8.73 (d, 1H, $J=4.0\text{Hz}$), 8.48 (m, 2H), 8.20 (d, 1H, $J=8.0\text{Hz}$), 8.09 (s, 1H), 7.99 (m, 1H), 7.88 (m, 1H), 7.38 (m, 1H), 7.05 (s, 1H), 6.81 (d, 1H, $J=8.0\text{Hz}$), 3.35 (m, 2H), 1.79 (m, 2H), 1.51-1.46 (m, 2H), 1.36-1.26 (m, 8H), 0.90 (m, 3H). ^{13}C NMR (125 MHz. CDCl_3): 155.54, 155.23, 151.82, 149.32, 145.26, 139.61, 137.02, 131.27, 130.46, 127.12, 124.14, 121.48, 120.42, 119.36, 117.96, 116.81, 92.32, 90.19, 43.17, 31.78, 29.25, 29.17, 28.93, 27.07, 22.64, 14.08. EI-TOF-HRMS $[(\text{C}_{26}\text{H}_{28}\text{N}_4\text{O}_2)^+]$: calcd. 428.2212; found 428.2223.

Synthesis of compound L-1: A solution of 5 (180mg, 0.42 mmol), zinc (138 mg, 2.1 mmol), and NH_4Cl (228mg, 4.2 mmol) in MeOH (15 mL) and water (8 mL) was stirred at 45°C for 3 h. The insoluble material was removed by filtration and neutralized sated NaHCO_3 solution. The mixture was concentrated and extracted with CH_2Cl_2 . The organic layer was separated, washed with water and brine, dried over Na_2SO_4 , and concentrated under vacuum to give the compound as a dark yellow solid (165.7mg). Then dark yellow solid (140mg) was added to the

suspension of alloxan monohydrate (60.6mg) and boric acid (21.3mg) in 20 mL of glacial acetic acid. The mixture was stirred overnight. Then the solution was concentrated under vacuum. The residue was purified by column chromatography (Al_2O_3 , CH_2Cl_2 : Methanol = 20:1, v/v). The compound 6 was collected as a tangerine solid (71.3mg, yield=33.7%). ^1H NMR (400MHz, DMSO-d₆): δ 11.44 (s, 1H), 8.98 (s, 1H), 8.74 (d, 1H, J =4.0Hz), 8.51 (d, 1H, J =8.0Hz), 8.44 (d, 1H, J =8.0Hz), 8.21 (m, 1H), 8.00 (m, 1H), 7.82 (d, 1H, J =8.0Hz), 7.52 (m, 1H), 4.59 (m, 2H), 1.75 (m, 2H), 1.50-1.45 (m, 2H), 1.29-1.23 (m, 8H), 0.85 (m, 3H). ^{13}C NMR (125 MHz, DMSO-d₆): δ 158.99, 154.89, 151.99, 150.53, 149.25, 139.83, 137.44, 137.33, 135.60, 133.54, 132.89, 130.76, 129.76, 121.83, 120.64, 117.90, 93.37, 92.06, 45.57, 31.93, 31.75, 29.70, 29.37, 29.25, 29.15, 27.12, 26.87, 22.69, 22.62, 14.11. MALDI-TOF-HRMS ([C₃₀H₂₈N₆O₂]⁺) : calcd. 504.2274; found 504.2289.

Synthesis of compound Ru-1: [RuCl₂(cymene)]₂ (37mg, 0.06mmol) and ligands (60.5mg, 0.12mmol) were suspended in ethanol (5.0 mL). The mixture was stirred at r.t. under N₂ atmosphere for ca. 2 h until the solution become clear. Then a solution of 2, 2'-bipyridine (37.5mg, 0.24mmol) in water (10 mL) was added and the mixture was refluxed for 22 h. After cooling, the solvent was evaporated under reduced pressure. The crude product was then subjected to column chromatography (silica gel eluted, acetonitrile : water : saturated aqueous KNO₃ = 100 : 9 : 1, v/v) and treated with a saturated aqueous solution of NH₄PF₆. Red precipitate was collected with filtration; the solid was washed with water and dried in a vacuum. Ru-1 was collected (21mg, yield=15%). ^1H NMR (400MHz, CD₃CN): δ 9.30 (s, 1H), 8.57-8.49 (m, 6H), 8.23 (d, 1H, J =8Hz), 8.13-8.04 (m, 6H), 7.96 (s, 1H), 7.86-7.83 (m, 2H), 7.76-7.71 (m, 3H), 7.68 (d, 1H, J =8Hz), 7.62 (d, 1H, J =12Hz), 7.44-7.40 (m, 5H), 4.55 (m, 2H), 1.76 (m, 2H), 1.50-1.46 (m, 2H),

1.40-1.24 (m, 8H), 0.87 (q, 3H). ^{13}C NMR (125MHz. CD_3CN): δ 158.97, 156.72, 156.67, 156.63, 156.51, 156.04, 154.83, 153.29, 151.68, 151.63, 151.52, 151.50, 151.28, 150.72, 139.71, 138.87, 137.70, 137.66, 137.59, 135.33, 132.71, 132.45, 128.32, 127.64, 127.55, 127.41, 127.39, 127.37, 127.28, 124.69, 124.13, 124.04, 124.02, 123.74, 122.56, 118.89, 94.33, 88.20, 44.61, 31.22, 28.67, 28.59, 26.15, 26.06, 22.07, 13.10. MALDI-TOF-HRMS ($[\text{C}_{50}\text{H}_{44}\text{N}_{10}\text{O}_2\text{Ru}]^+$) : calcd. 918.2692; found 918.2717.

Synthesis of compound 6: 4 (220mg, 0.67 mmol) and trimethylsilylacetylene (646mg, 6.7mmol) was dissolved in 15 mL of dried Et_3N under N_2 . $(\text{PPh}_3)_4\text{Pd}$ (38 mg, 0.033 mmol) and CuI (12 mg, 0.066mmol) were added before the mixture was stirred for 8-12 h at 89 °C. After the reaction was finished, the solvent was removed under reduced pressure. The residue was purified by column chromatography (silica gel, CH_2Cl_2 : Petroleum ether = 1 : 5, v/v). 6 was collected as a dark yellow solid (123 mg, 52.6%). ^1H NMR (400MHz, CDCl_3): δ 8.10 (d, 1H, $J=8.0\text{Hz}$), 8.01 (s, 1H), 6.92 (s, 1H), 6.67 (d, 1H, $J=8\text{Hz}$), 3.29 (m, 3H), 1.75-1.71 (m, 3H), 1.47-1.44 (m, 2H), 1.33-1.29 (m, 8H), 0.89 (m, 3H), 0.27 (s, 9H). ^{13}C NMR (125MHz. CDCl_3): 145.44, 131.35, 131.21, 127.09, 118.55, 117.31, 103.91, 99.37, 43.33, 32.01, 31.13, 29.47, 29.41, 29.16, 27.28, 22.88, 14.32. EI-TOF-HRMS ($[\text{C}_{19}\text{H}_{30}\text{N}_2\text{O}_2\text{Si}]^+$): calcd. 346.2077; found 346.2087.

Synthesis of compound 7: A solution of 6 (100 mg, 0.28 mmol), zinc (91 mg, 1.4 mmol), and NH_4Cl (150 mg, 2.8 mmol) in MeOH (4 mL) and water (2 mL) was stirred at 45°C for 3 h. The insoluble material was removed by filtration and neutralized satd NaHCO_3 solution. The mixture was concentrated and extracted with ethyl acetate. The organic layer was separated, washed with water and brine, dried over Na_2SO_4 , and concentrated under vacuum. The liquid was purified by colu

mn chromatography (silica gel, CH₂Cl₂ : Petroleum ether = 1 : 1, v/v). 7 was collected as a dark yellow solid (73 mg, 82.0%). ¹H NMR (400MHz, CDCl₃): δ 6.84 (d, 1H, J=8Hz), 6.77 (s, 1H), 6.59 (d, 1H, J=8Hz), 3.08 (m, 2H), 1.66 (m, 2H), 1.44-1.40 (m, 2H), 1.33-1.26 (m, 8H), 0.89 (m, 3H), 0.23 (s, 9H). ¹³C NMR (125MHz, CDCl₃): δ 136.87, 135.24, 123.24, 115.41, 115.19, 114.26, 106.58, 90.74, 44.18, 31.65, 29.51, 29.42, 29.24, 29.07, 27.09, 22.48, 13.90. LTQ–Orbitrap–HRMS ([C₁₉H₃₂N₂Si+H]⁺): calcd. 317.2413, found 317.2412.

Synthesis of compound 8: Compound 7 (55mg, 0.17 mmol) was added dropwise to the suspension of alloxan monohydrate (29mg, 0.2 mmol) and boric acid (11mg, 0.17 mmol) in 20 mL of glacial acetic acid. The mixture was stirred overnight. The solvent was removed under reduced pressure. The residue was purified by column chromatography (silica gel, CH₂Cl₂ : ethyl acetate = 7:1, v/v). 7 was collected as a yellow solid (51 mg, 69.8%). ¹H NMR (400MHz, CDCl₃): δ 8.79 (s, 1H), 8.23 (d, 1H, J=8Hz), 7.64 (d, 2H, J=8Hz), 4.66 (m, 2H), 1.87 (m, 2H), 1.43-1.41 (m, 2H), 1.34-1.26 (m, 8H), 0.89 (m, 3H), 0.33 (s, 9H). ¹³C NMR (125MHz, CDCl₃): δ 159.41, 155.38, 150.83, 137.65, 135.79, 133.61, 133.04, 131.60, 130.46, 118.51, 103.45, 45.80, 32.07, 30.04, 29.53, 29.46, 27.40, 27.12, 22.94, 14.41. LTQ–Orbitrap–HRMS ([C₂₃H₃₀N₄O₂Si+H]⁺): calcd. 423.2216, found 423.2212.

Synthesis of compound EFL: 8 (30 mg, 0.07 mmol) was dissolved in 3 mL distilled THF. Bu₄NF (46.5mg, 0.18mmol) was added under N₂ and the solution was kept at 0°C for about 1 h (monitored by TLC until the starting material had been completely consumed). After the reaction was finished, 20 mL water and 30 ml CH₂Cl₂ was added. The aqueous layer was extracted with CH₂Cl₂ (3 × 10 mL). The combined organic layers were dried over anhydrous Na₂SO₄. The solvent was removed under reduced pressure. The residue was purified by column chromatography (silica gel, CH₂

Cl_2 : PE = 1 : 4, v/v). EFL was collected as a yellow solid (18 mg, yield: 69.8 %). ^1H NMR (400MHz, CDCl_3): δ 8.69 (s, 1H), 8.26 (d, 1H, $J=8\text{Hz}$), 7.68 (d, 2H, $J=8\text{Hz}$), 4.65 (m, 2H), 3.53 (s, 1H), 1.85 (m, 2H), 1.53-1.51 (m, 2H), 1.40-1.25 (m, 8H), 0.88 (m, 3H). ^{13}C NMR (125MHz. CDCl_3): δ 158.86, 154.74, 150.45, 137.71, 135.58, 133.45, 132.65, 130.15, 129.99, 118.75, 83.98, 82.09, 45.58, 31.72, 29.20, 29.12, 27.08, 26.82, 22.61, 14.06. EI-TOF-HRMS ($[\text{C}_{20}\text{H}_{22}\text{N}_4\text{O}_2]^+$): calcd. 350.1743, found 350.1747.

Synthesis of compound 9: The synthesis route is similar to the route of compound 4. 9 was collected as a yellow liquid (16 mg, yield: 98.5 %). ^1H NMR (400MHz, CDCl_3): δ 8.17 (s, 1H), 8.15 (s, 1H), 7.42 (m, 1H), 6.84 (m, 1H), 6.62 (m, 1H), 3.29 (m, 2H), 1.74 (m, 2H), 1.34-1.31 (m, 2H), 1.30-1.26 (m, 8H), 0.89 (m, 3H). ^{13}C NMR (125MHz. CDCl_3): δ 145.62, 136.15, 131.67, 126.81, 114.97, 113.78, 43.04, 31.79, 29.28, 29.20, 28.97, 27.09, 22.65, 14.08. LTQ-Orbitrap-HRMS ($[\text{C}_{14}\text{H}_{22}\text{N}_2\text{O}_2+\text{H}]^+$): calcd. 251.1760, found 251.1757.

Synthesis of compound 10: The synthesis route is similar to the route of compound 7. (42 mg, 95%). ^1H NMR (400MHz, CDCl_3): δ 6.82 (m, 1H), 6.67 (m, 3H), 3.24 (s, 3H), 3.08 (m, 2H), 1.68-1.62 (m, 2H), 1.45-1.39 (m, 2H), 1.33-1.26 (m, 8H), 0.89 (m, 3H). ^{13}C NMR (125MHz. CDCl_3): δ 138.20, 134.01, 120.76, 118.28, 116.46, 111.60, 44.30, 31.85, 29.75, 29.48, 29.29, 27.33, 22.67, 14.10. LTQ-Orbitrap-HRMS ($[\text{C}_{14}\text{H}_{24}\text{N}_2+\text{H}]^+$): calcd. 221.2018, found 221.2018.

Synthesis of compound FL: The synthesis route is similar to the route of compound 8. FL was collected as a yellow solid (30mg, yield: 42 %). ^1H NMR (400MHz, CDCl_3): δ 8.52 (s, 1H), 8.34 (s, 1H), 7.94 (m, 1H), 7.66 (m, 2H), 4.71 (m, 2H), 1.88 (m, 2H), 1.55-1.50 (m, 2H), 1.42-1.26 (m, 8H), 0.89 (m, 3H). ^{13}C NMR (125MHz. CDCl_3): δ 159.12, 155.00, 150.32, 137.52, 136.11, 135.97, 133.64,

132.71, 126.79, 115.37, 45.61, 31.72, 29.28, 29.15, 27.20, 26.92, 22.60, 14.05. EI-TOF-HRMS ([C₁₈H₂₂N₄O₂]⁺): calcd. 326.1743, found 326.1745.

3. NMR and HRMS Spectra

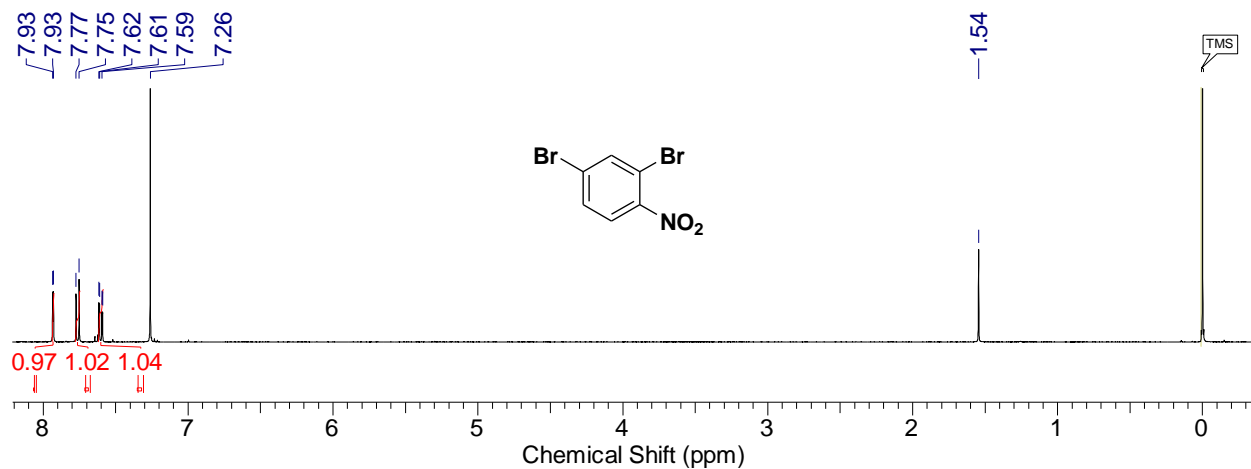


Figure S1. ¹H NMR spectrum of **3** (400 MHz, CDCl₃), 25 °C.

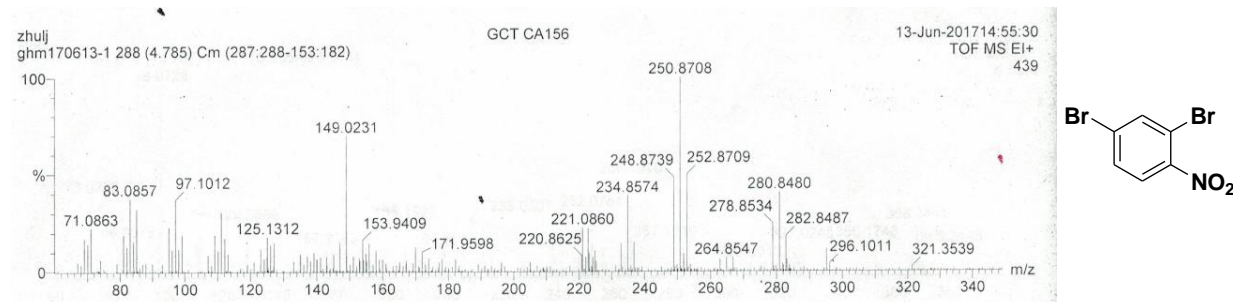


Figure S2. EI-TOF-HRMS spectrum of **3**.

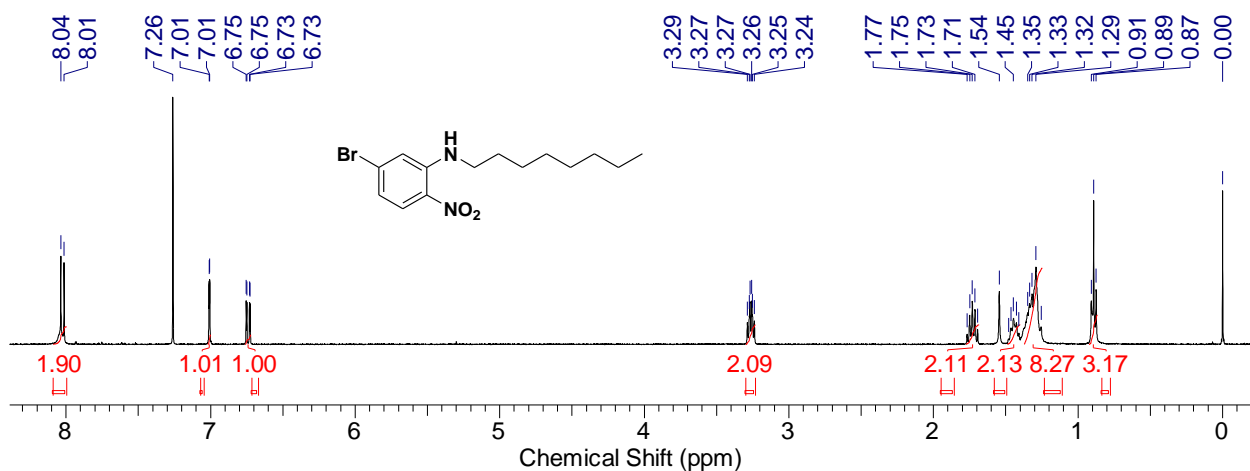


Figure S3. ^1H NMR spectrum of **4** (400 MHz, CDCl_3), 25 °C.

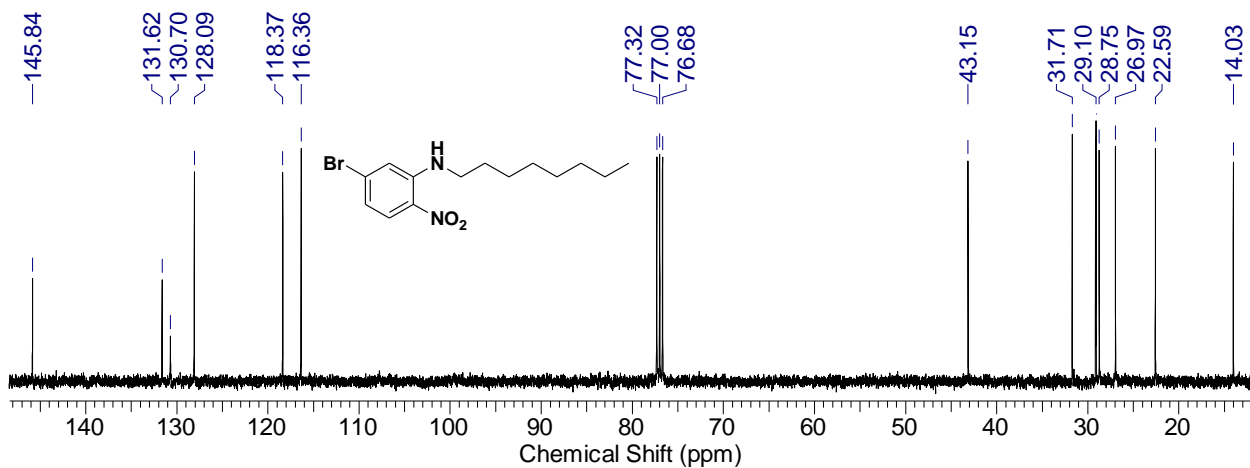


Figure S4. ^{13}C NMR spectrum of **4** (400 MHz, CDCl_3), 25 °C.

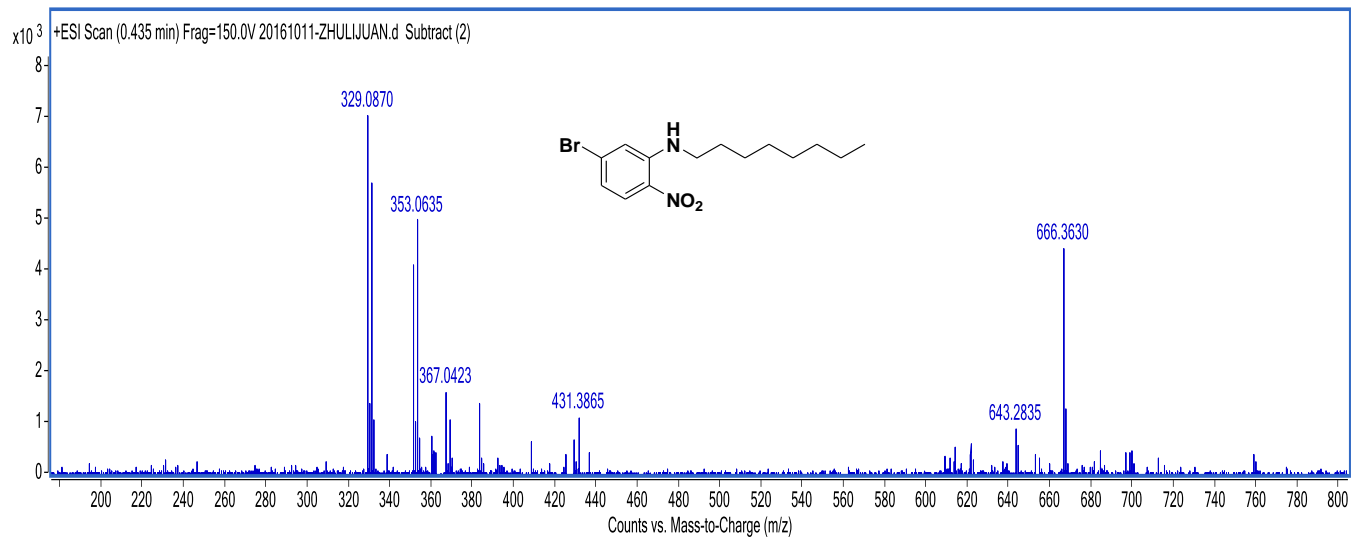


Figure S5. ESI–MOF–HRMS spectrum of **4**.

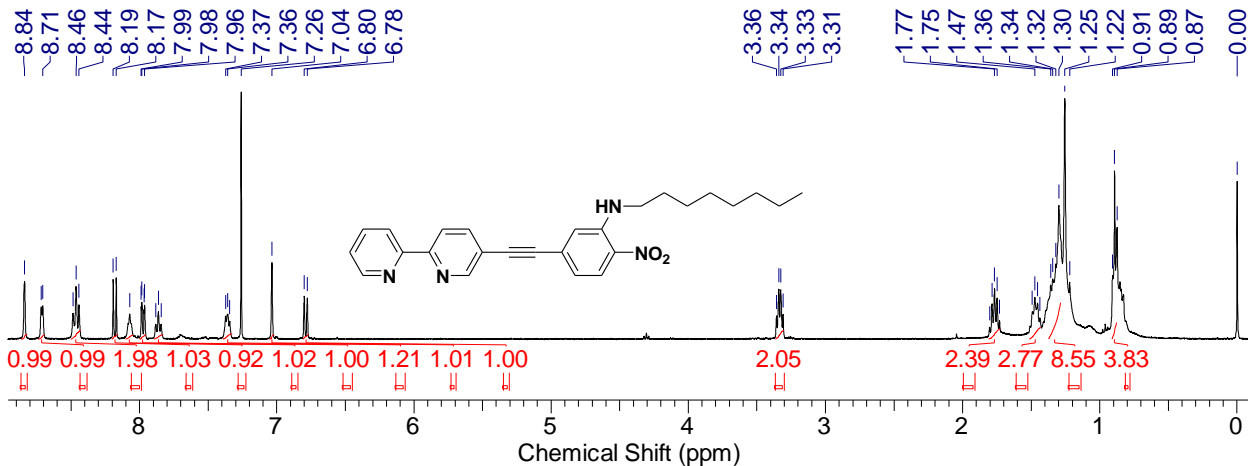


Figure S6. ^1H NMR spectrum of **5** (400 MHz, CDCl_3), 25 °C.

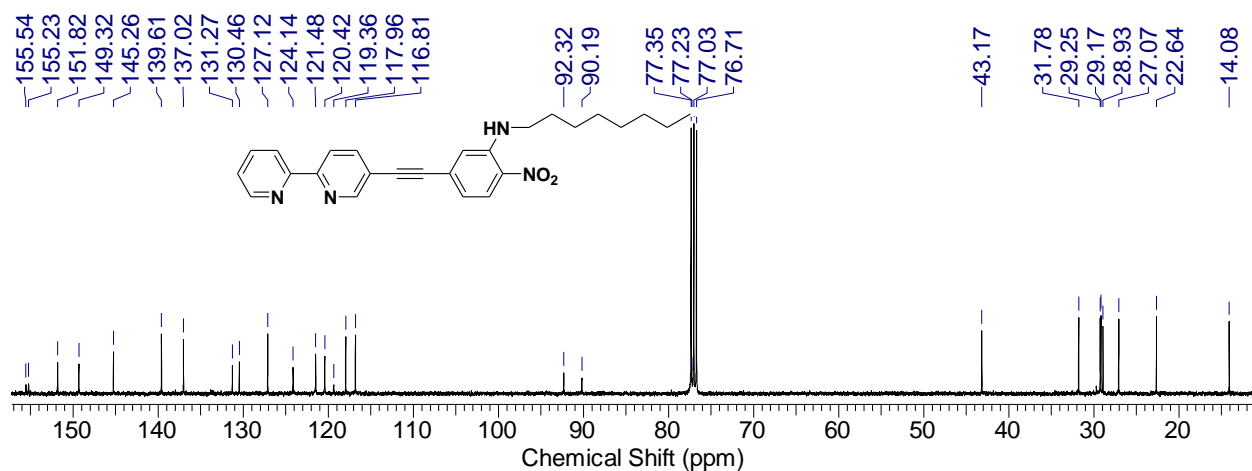


Figure S7. ^{13}C NMR spectrum of **5** (400 MHz, CDCl_3), 25 °C.

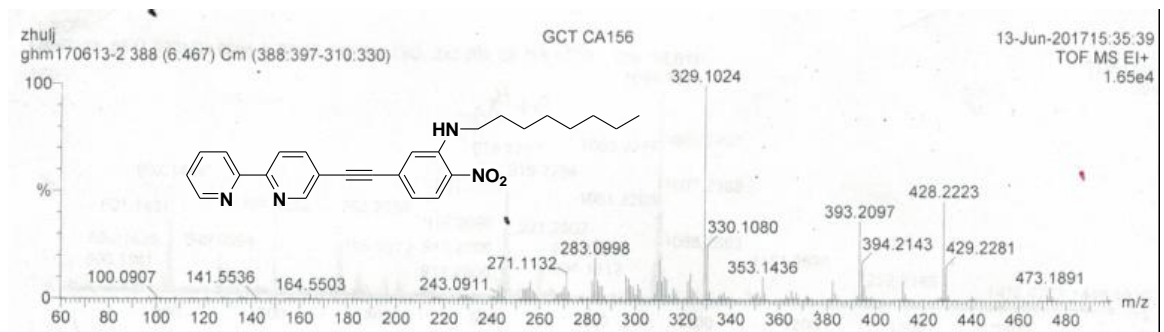


Figure S8. EI-TOF-HRMS spectrum of **5**.

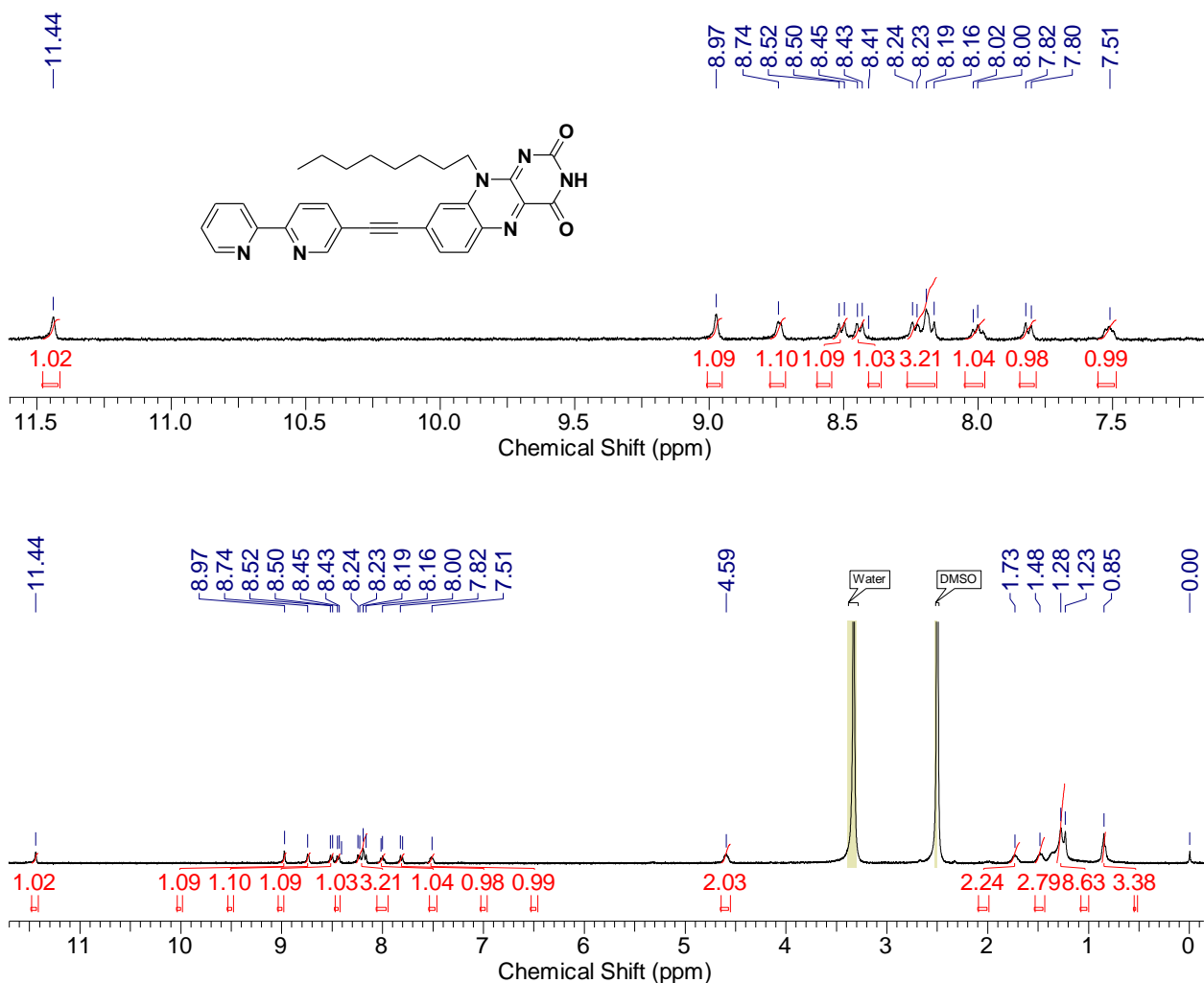


Figure S9. ^1H NMR spectrum of **L-1** (400 MHz, DMSO-d_6), 25 °C.

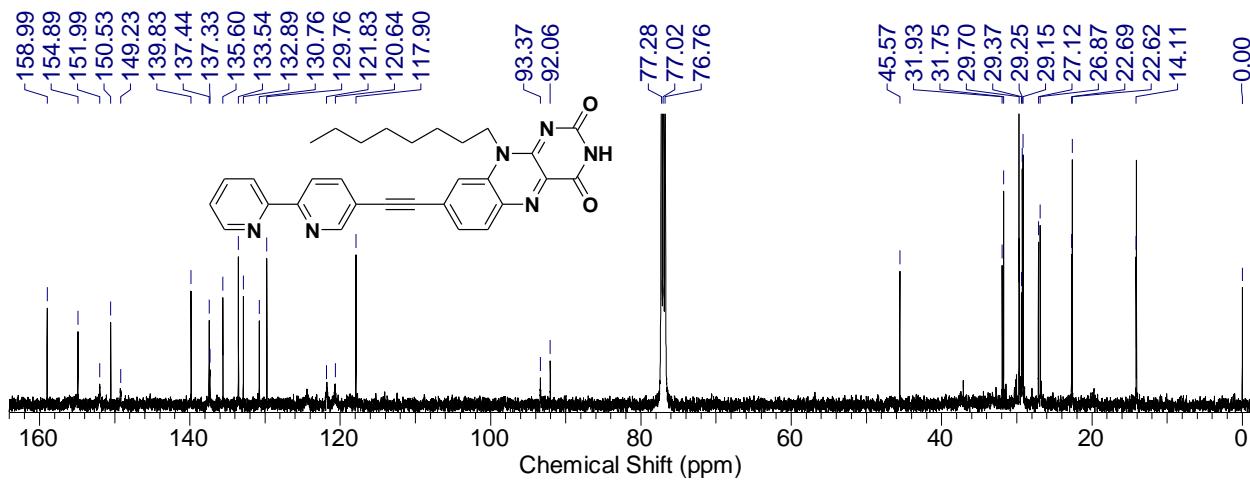


Figure S10. ¹³C NMR spectrum of L-1 (400 MHz, DMSO-d₆), 25 °C.

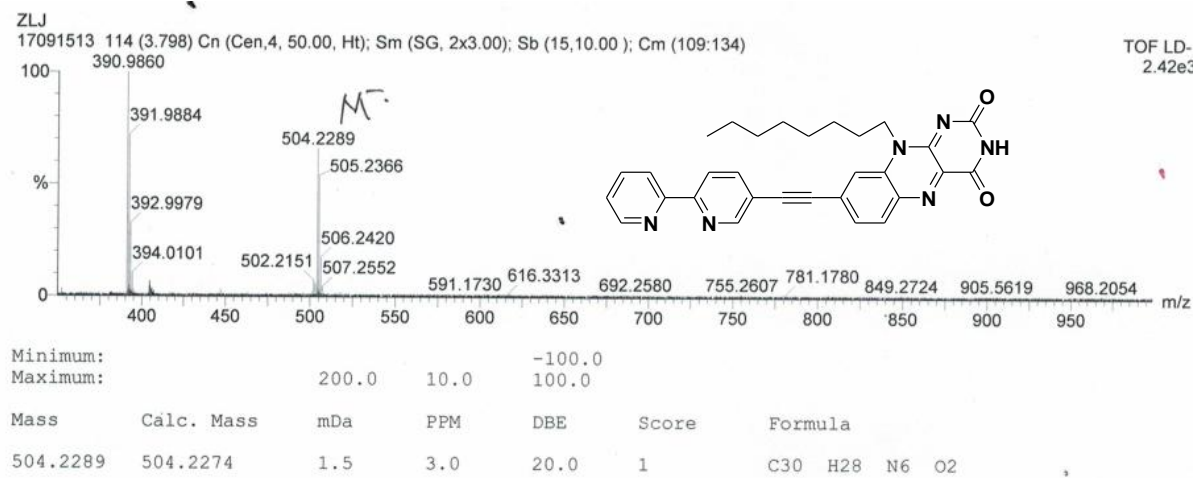


Figure S11. MALDI-TOF-HRMS spectrum of L-1

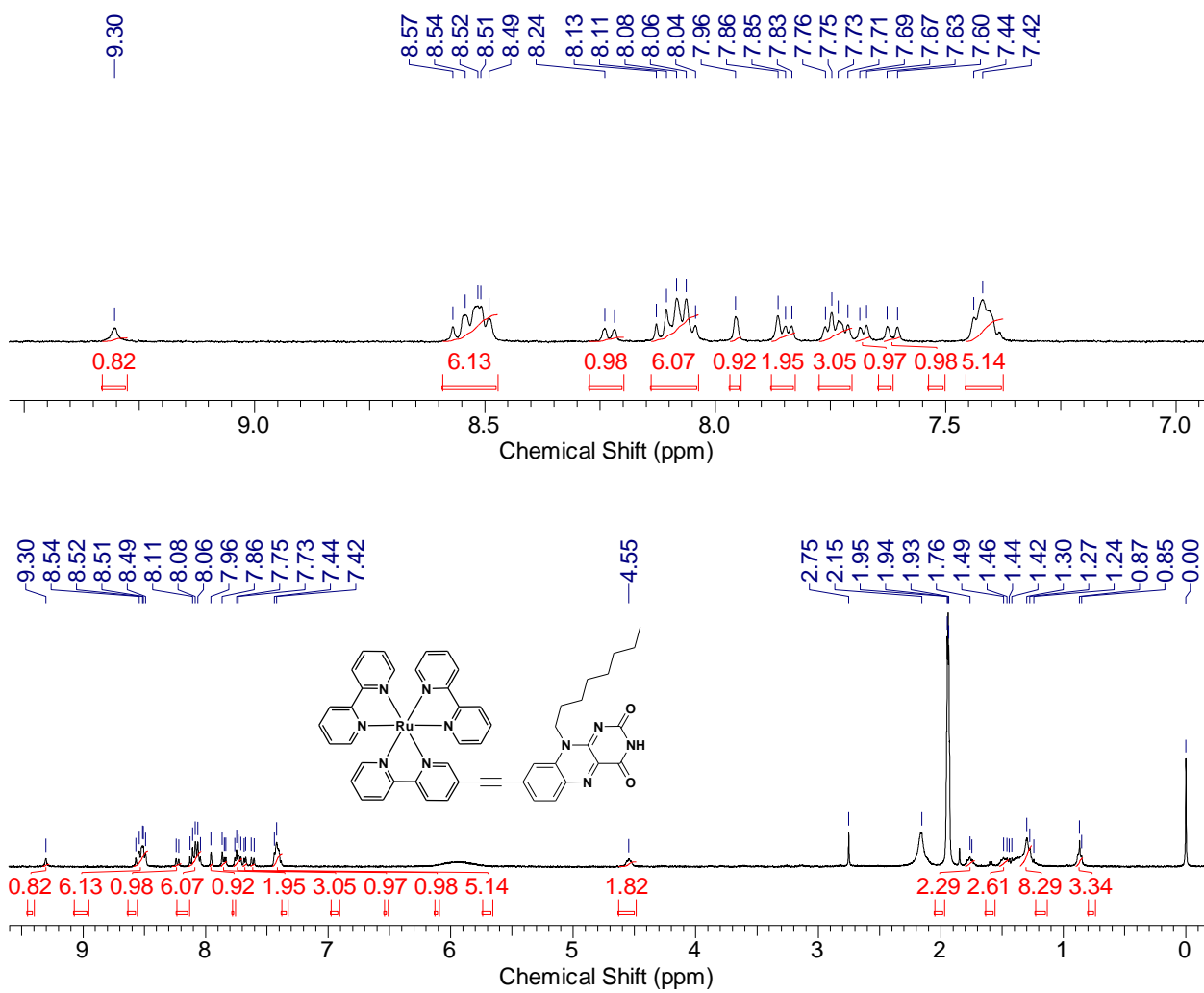


Figure S12. ^1H NMR spectrum of **Ru-1** (400 MHz, CD_3CN), 25 °C.

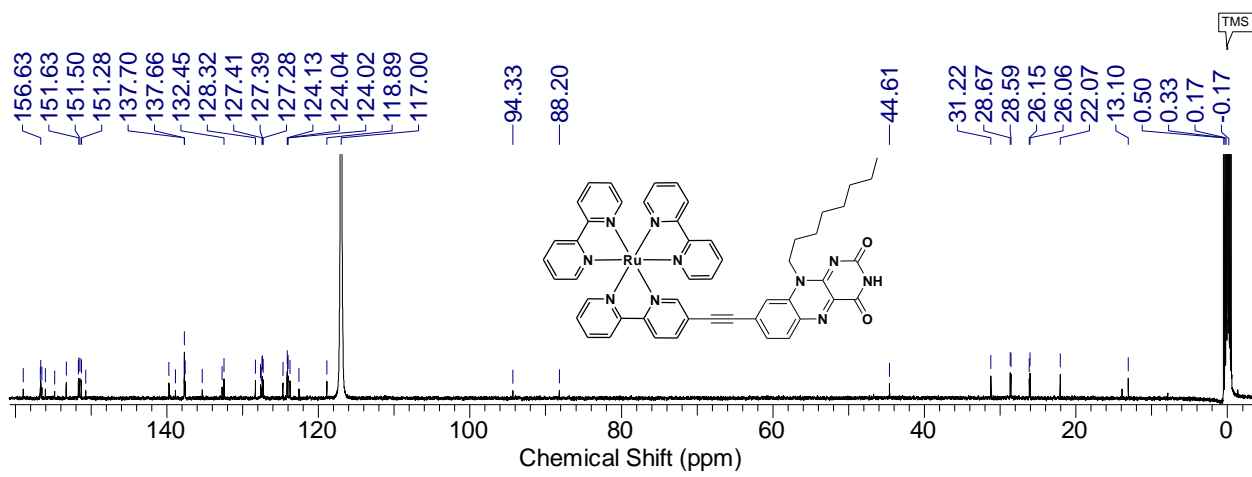


Figure S13. ^{13}C NMR spectrum of **Ru-1** (400 MHz, CD_3CN), 25 °C.

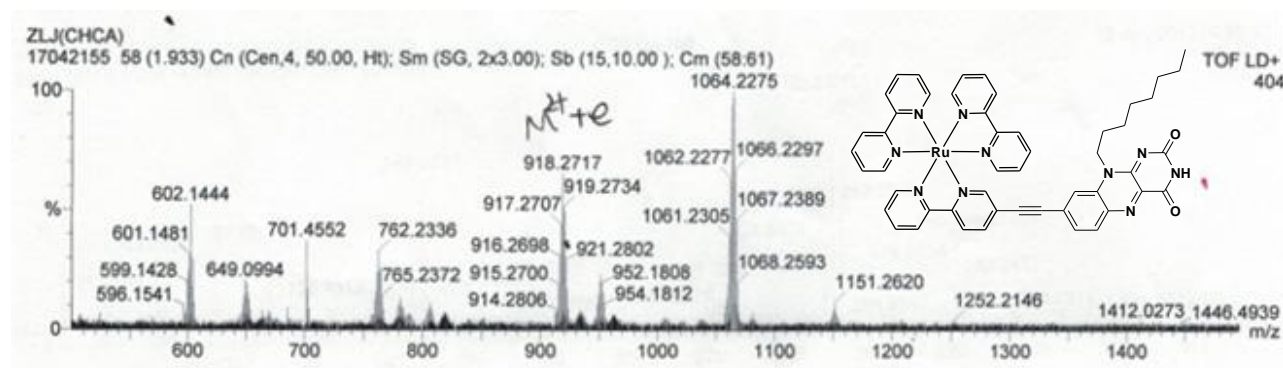


Figure S14. MALDI-TOF-HRMS spectrum of **Ru-1**

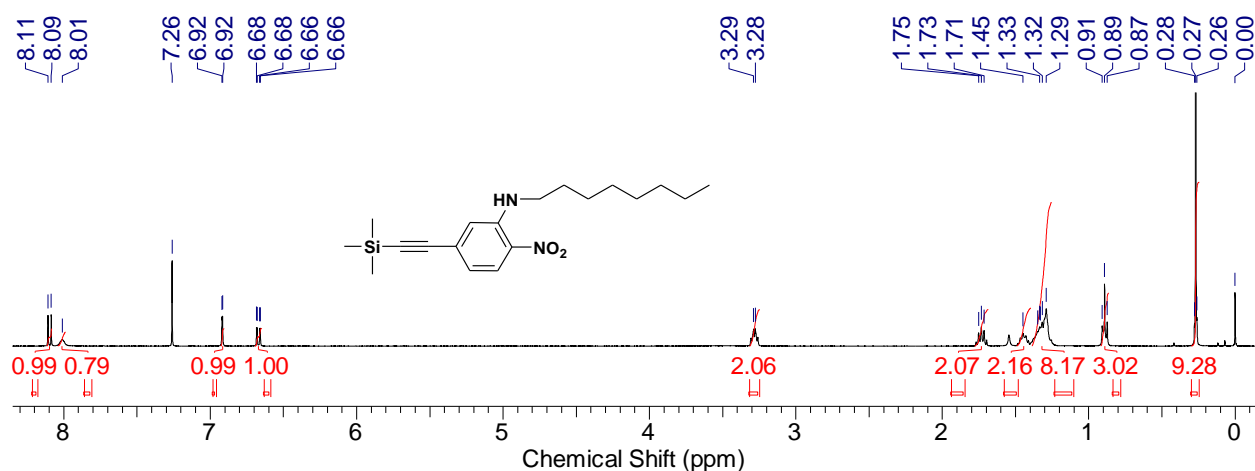


Figure S15. ^1H NMR spectrum of **6** (400 MHz, CDCl_3), 25 °C.

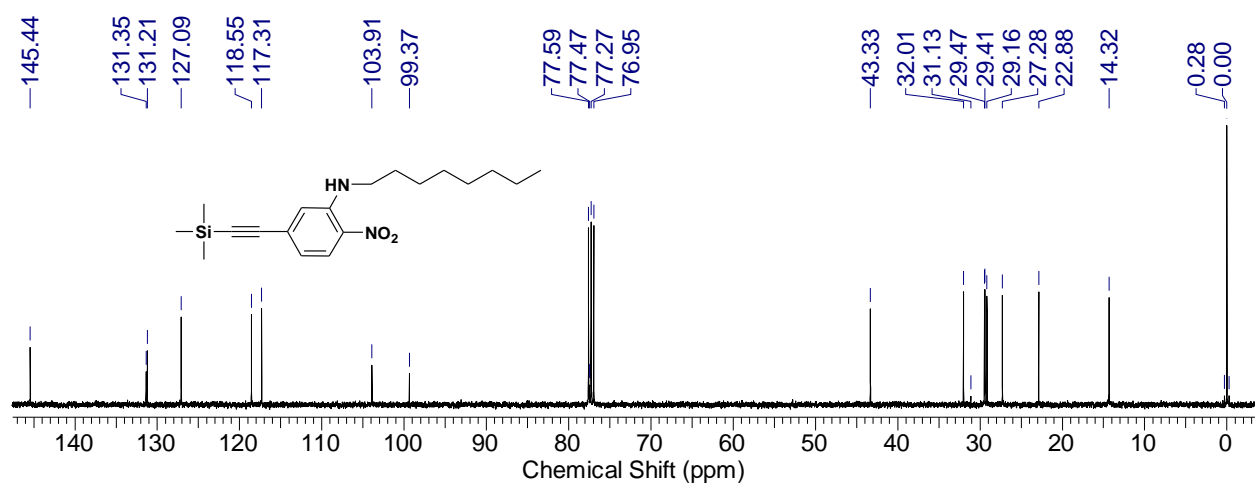


Figure S16. ^{13}C NMR spectrum of **6** (400 MHz, CDCl_3), 25 °C.

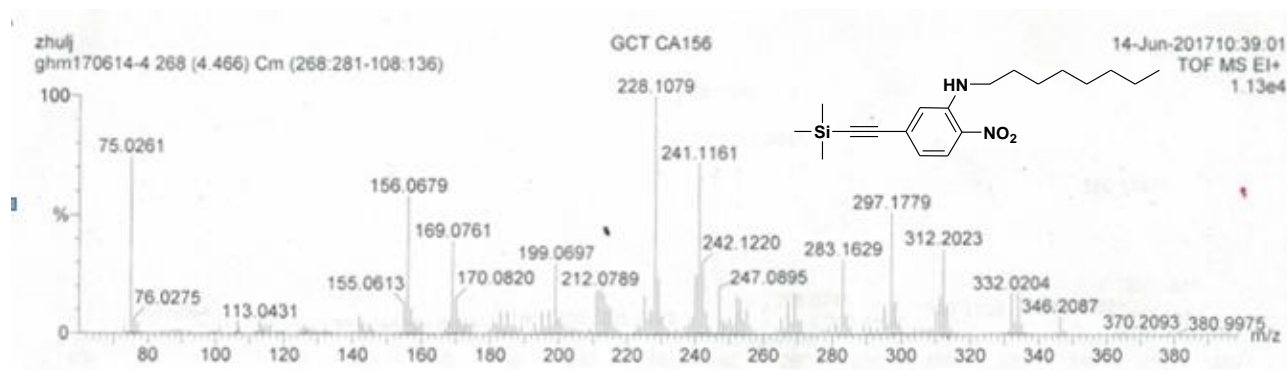


Figure S17. EI–TOF–HRMS spectrum of **6**.

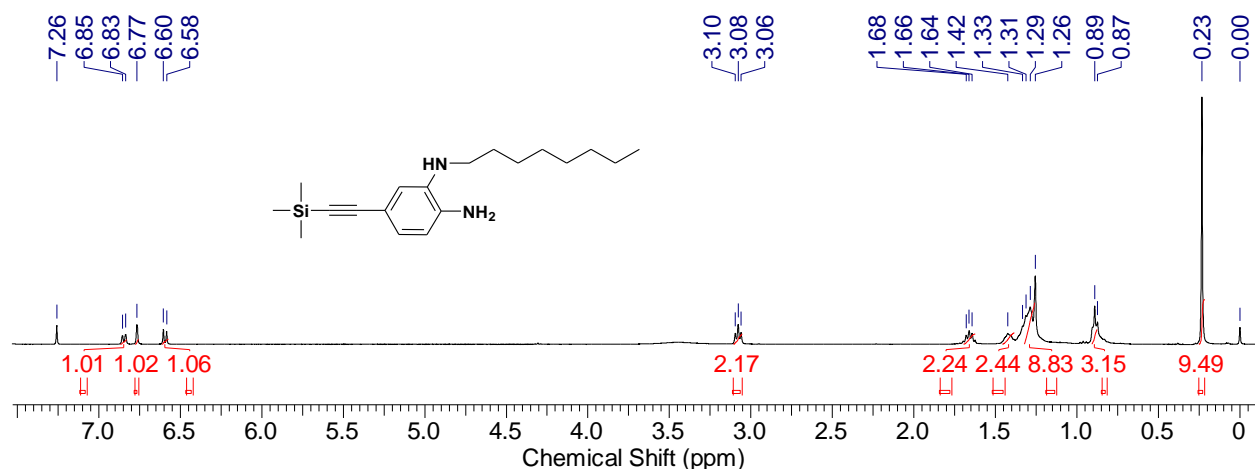


Figure S18. ^1H NMR spectrum of **7** (400 MHz, CDCl_3), 25 °C.

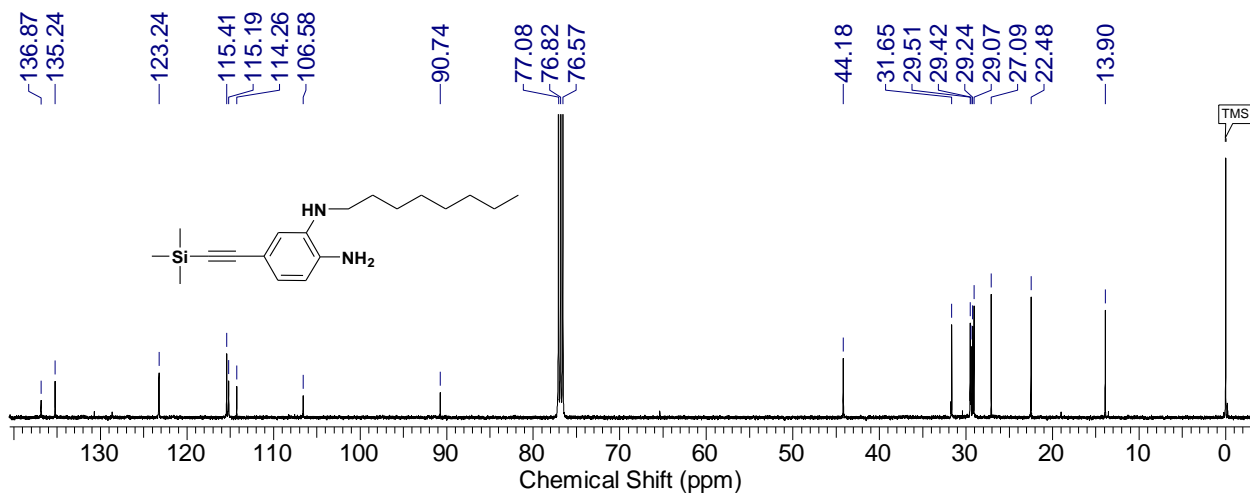


Figure S19. ^{13}C NMR spectrum of **7** (400 MHz, CDCl_3), 25 °C.

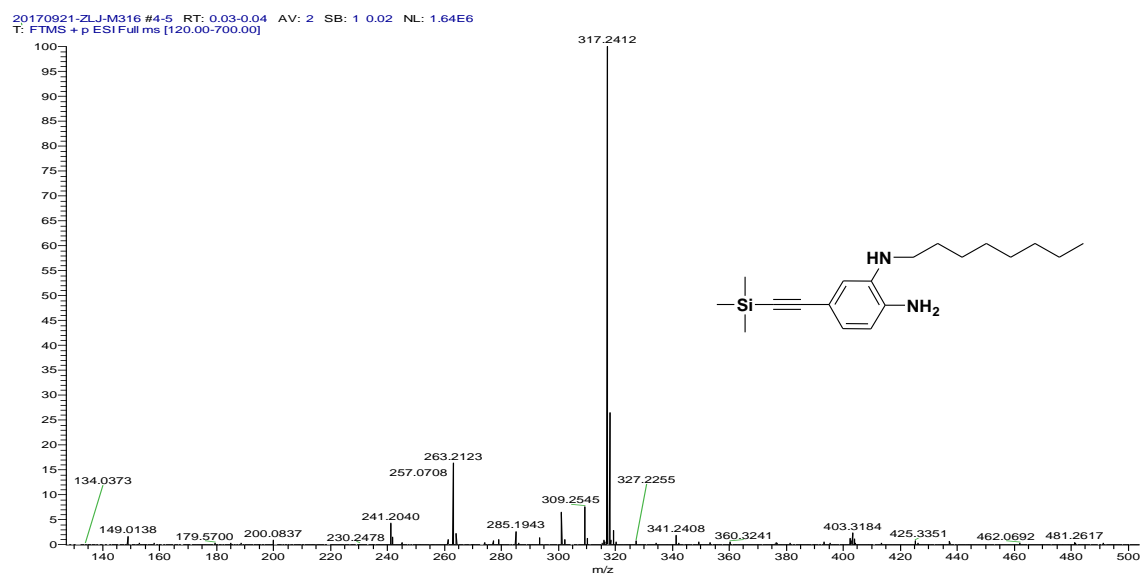


Figure S20. LTQ–Orbitrap–HRMS spectrum of **7**.

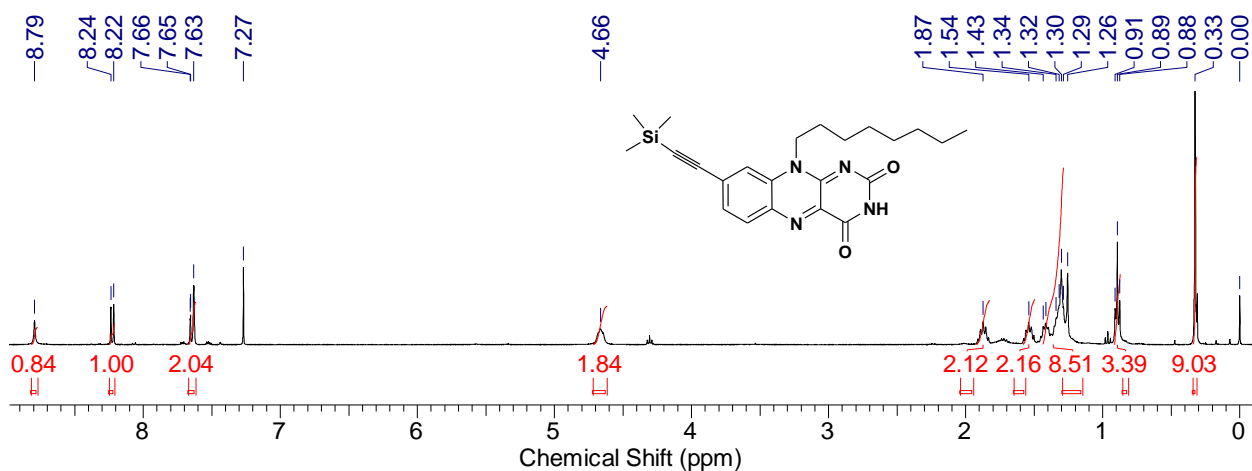


Figure S21. ^1H NMR spectrum of **8** (400 MHz, CDCl_3), 25 °C.

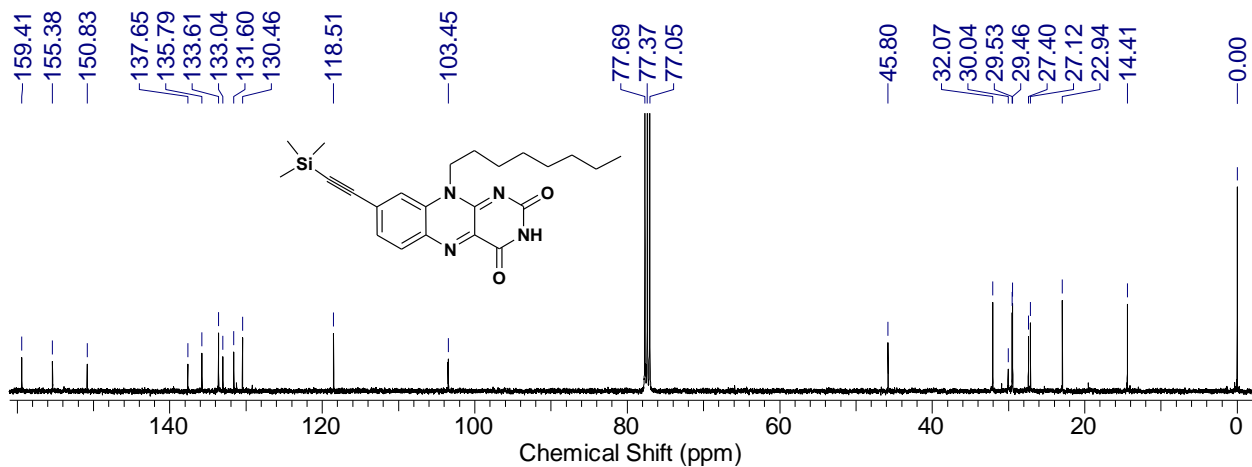


Figure S22. ^{13}C NMR spectrum of **8** (400 MHz, CDCl_3), 25 °C.

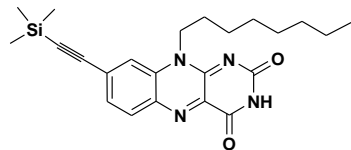
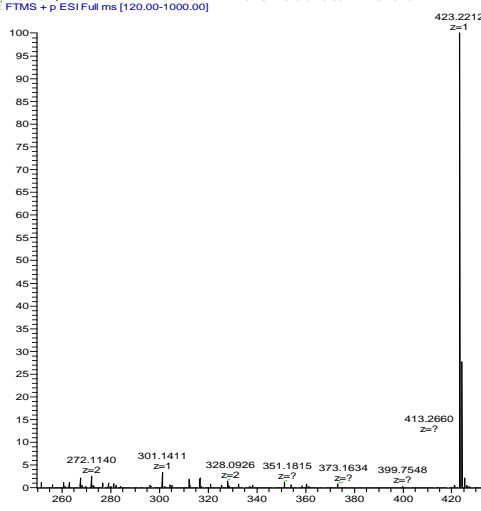
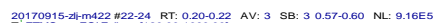


Figure S23. LTQ–Orbitrap–HRMS spectrum of **8**.

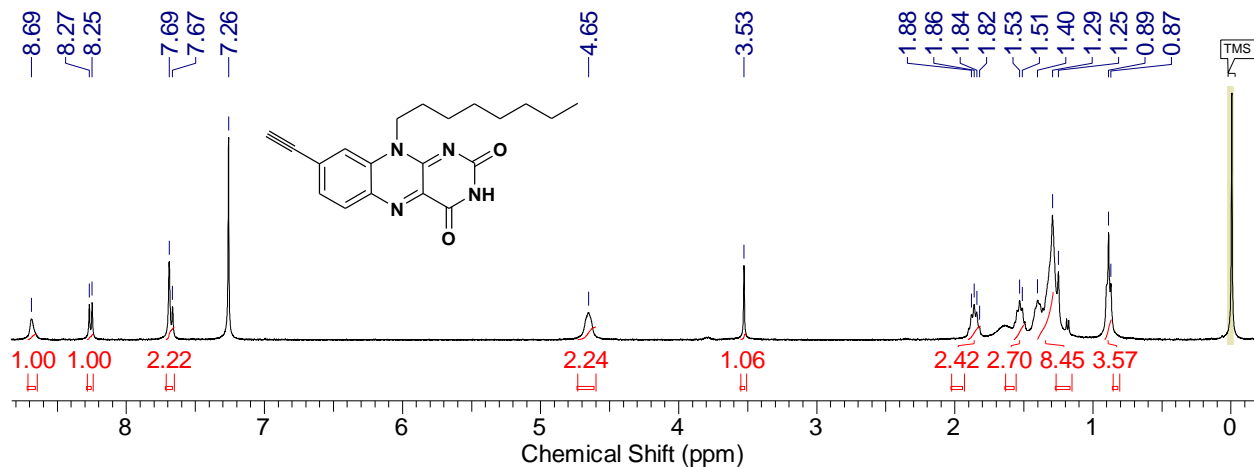


Figure S24. ^1H NMR spectrum of **EFL** (400 MHz, CDCl_3), 25 °C.

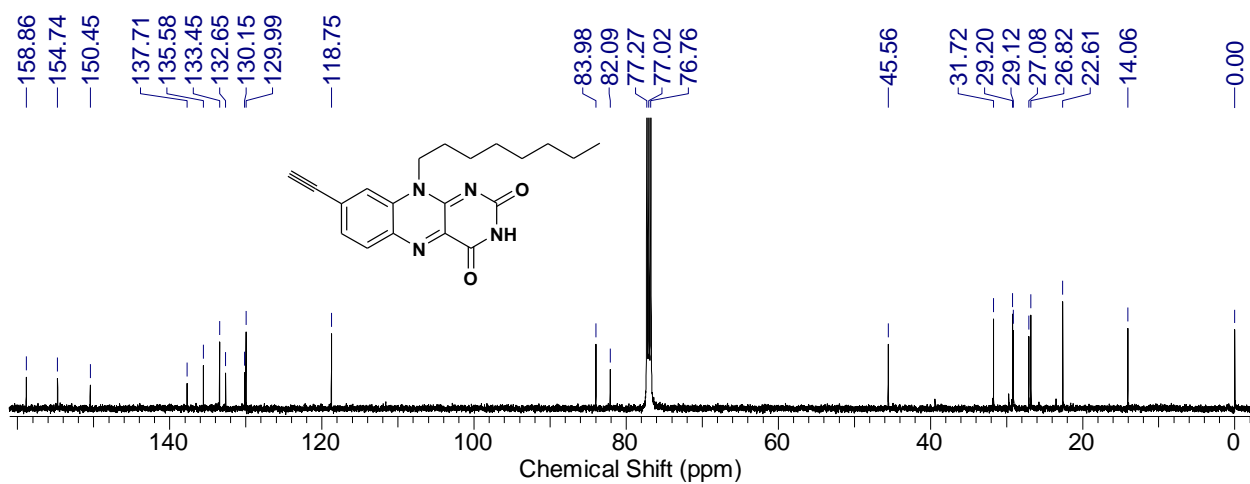


Figure S25. ^{13}C NMR spectrum of **EFL** (400 MHz, CDCl_3), 25 °C.

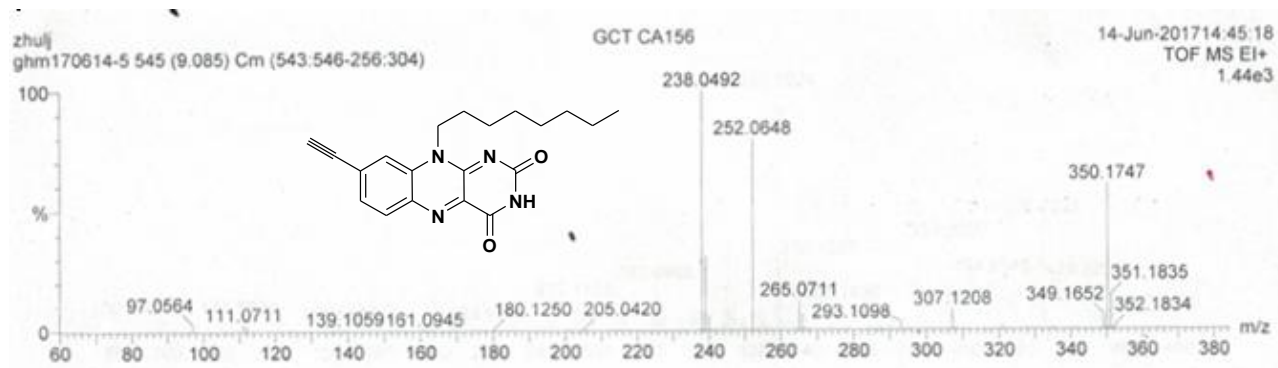


Figure S26. EI-TOF-HRMS spectrum of **EFL**.

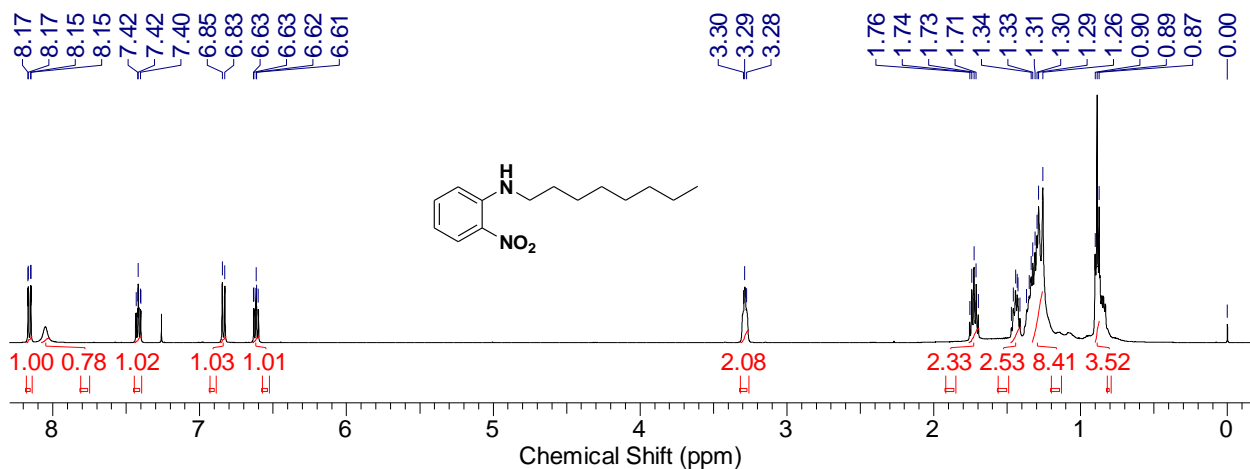


Figure S27. ^1H NMR spectrum of **9** (400 MHz, CDCl_3), 25 °C.

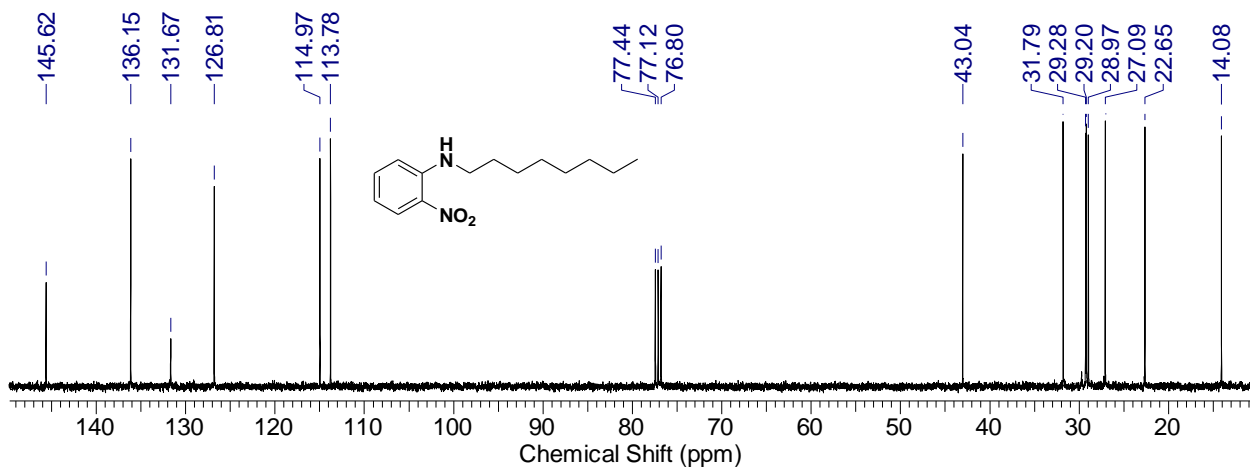


Figure S28. ^{13}C NMR spectrum of **9** (400 MHz, CDCl_3), 25 °C.

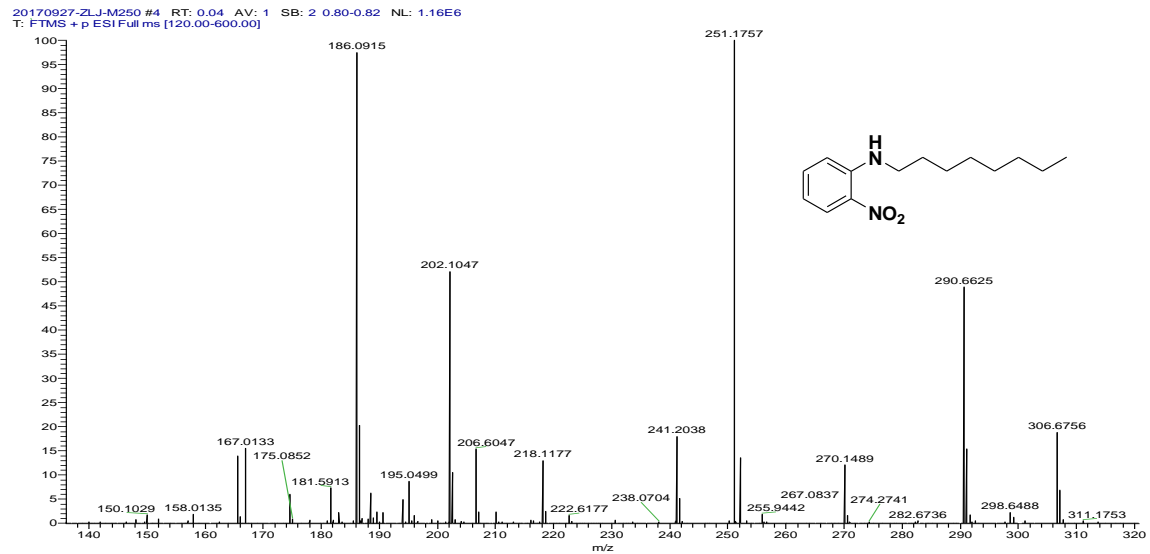


Figure S29. LTQ–Orbitrap–HRMS spectrum of **9**.

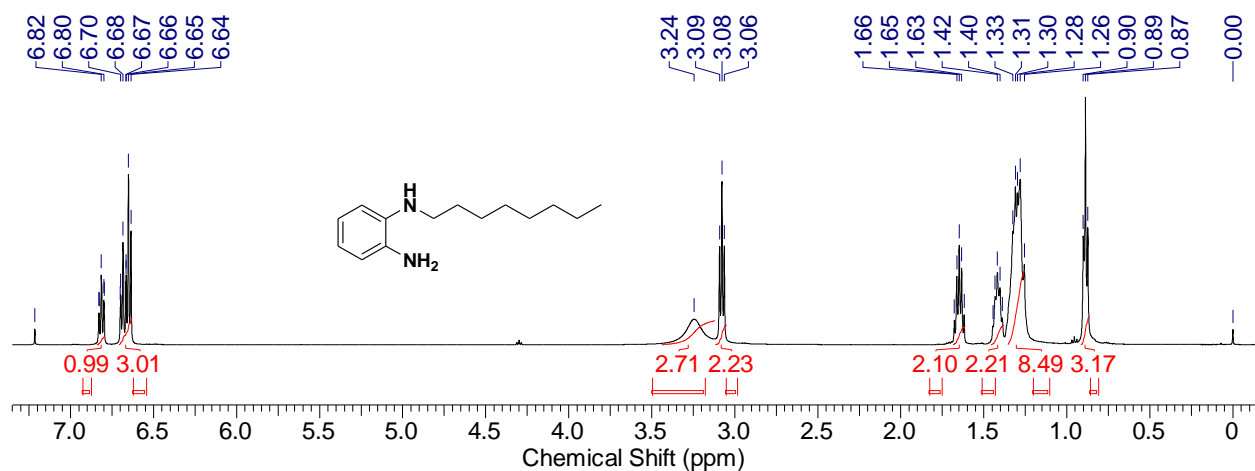


Figure S30. ^1H NMR spectrum of **10** (400 MHz, CDCl_3), 25 °C.

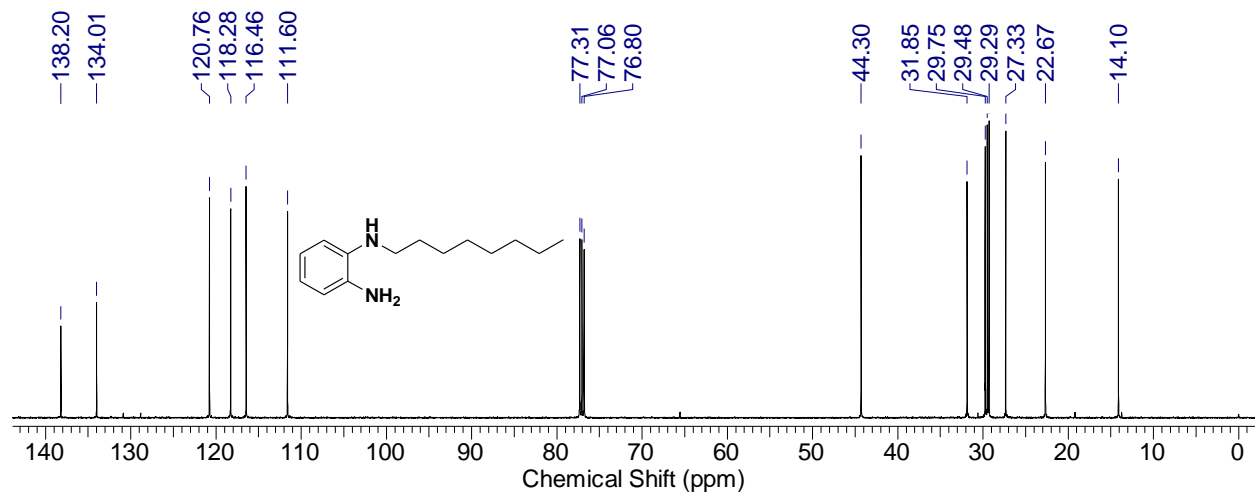


Figure S31. ^{13}C NMR spectrum of **10** (400 MHz, CDCl_3), 25 °C.

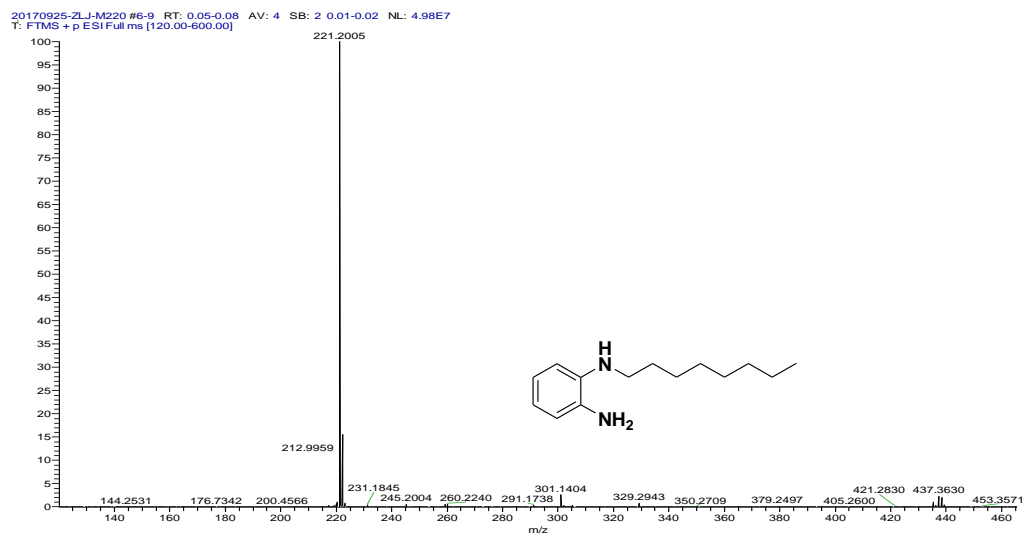


Figure S32. LTQ–Orbitrap–HRMS spectrum of **10**.

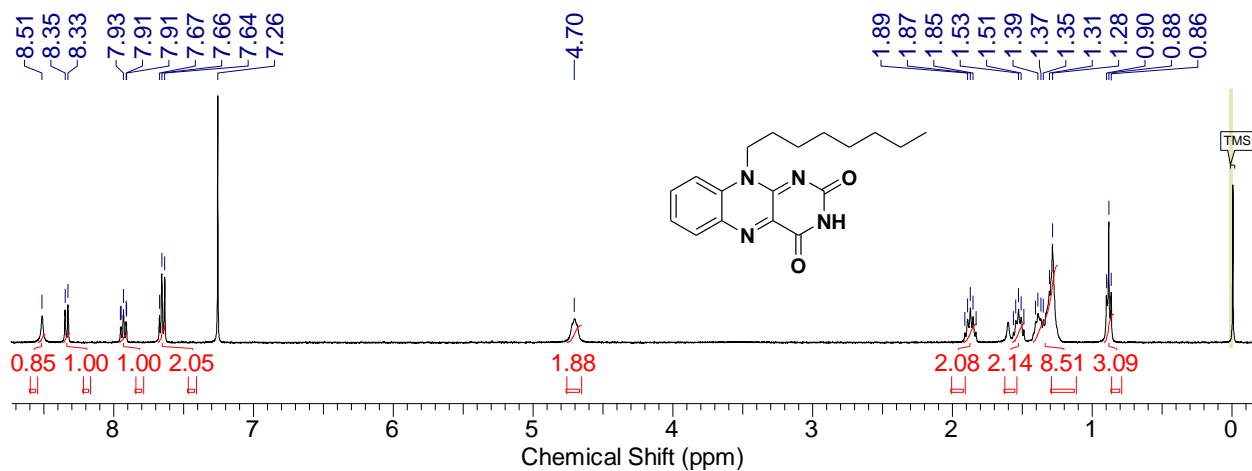


Figure S33. ^1H NMR spectrum of **FL** (400 MHz, CDCl_3), 25 °C.

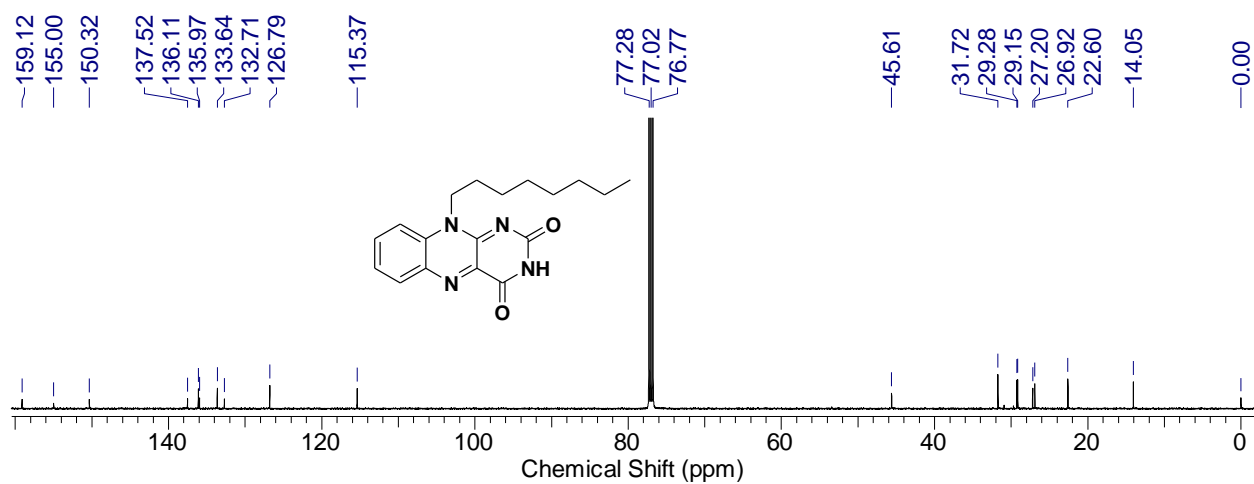


Figure S34. ^{13}C NMR spectrum of **FL** (400 MHz, CDCl_3), 25 °C.

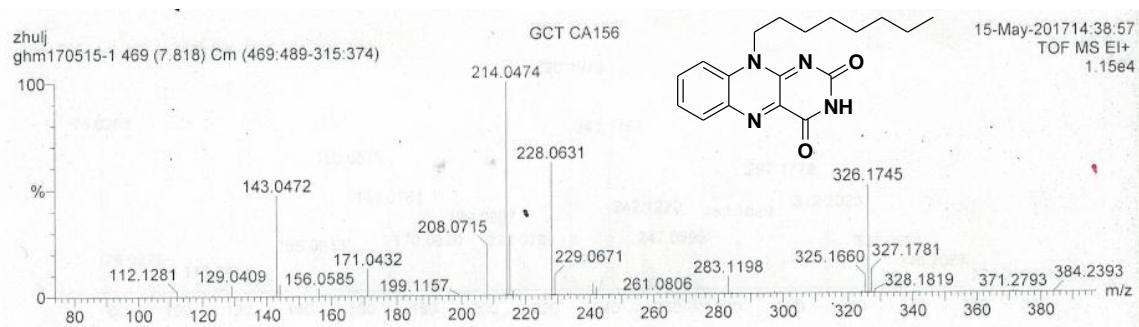


Figure S35. EI-TOF-HRMS spectrum of **FL**.

4. TD-DFT calculations and NTO analysis

Table S1. Electronic transitions involved in the excitation of Ru-1 in visible light region (Calculated with TD-B3LYP functional).^a

Transitions	Energy ^a	f ^b	Composition ^c	CI ^d	Character
$S_0 \rightarrow S_1$	2.3245 eV/533.38 nm	0.0189	194 -> 195	0.64339	M ->L', L ->L'
			194 -> 196	0.26961	M ->L', L ->L'
$S_0 \rightarrow S_2$	2.5073 eV/494.49 nm	0.0341	192 -> 195	0.19016	M ->L', L ->L'
			193 -> 195	0.62141	M ->L', L ->L'
			193 -> 196	0.24274	d ->d, L ->L'
$S_0 \rightarrow S_3$	2.5685 eV/482.71 nm	0.0435	191 -> 195	0.12279	L ->L', M ->L'
			192 -> 195	0.62775	M ->L', L ->L'
			192 -> 196	0.19108	d ->d, L ->L'
			193 -> 195	0.20520	M ->L', L ->L'
$S_0 \rightarrow S_4$	2.7277 eV/454.54 nm	1.0202	191 -> 195	0.67220	L ->L', M ->L'
			192 -> 195	0.14582	M ->L', L ->L'
$S_0 \rightarrow S_5$	2.7570 eV/449.70 nm	0.0089	194 -> 197	0.46658	M ->L', L ->L'
			194 -> 198	0.50370	M ->L', L ->L'
$S_0 \rightarrow S_6$	2.7649 eV/448.43 nm	0.0005	194 -> 196	0.15051	M ->L', L ->L'
			194 -> 197	0.48734	M ->L', L ->L'
			194 -> 198	0.47428	M ->L', L ->L'
$S_0 \rightarrow S_7$	2.8653 eV/432.72 nm	0.0002	194 -> 195	0.28180	M ->L', L ->L'
			194 -> 196	0.60559	M ->L', L ->L'
			194 -> 197	0.13433	M ->L', L ->L'
			194 -> 199	0.11061	d ->d, L ->L'
$S_0 \rightarrow S_8$	2.9480 eV/420.57 nm	0.0029	192 -> 198	0.43535	d ->d, L ->L'
			193 -> 197	0.46684	M ->L', L ->L'
			193 -> 198	0.26909	d ->d, L ->L'
$S_0 \rightarrow S_9$	2.9768 eV/416.51 nm	0.0021	192 -> 196	0.25036	d ->d, L ->L'
			192 -> 197	0.53215	M ->L', L ->L'

$S_0 \rightarrow S_{10}$	3.0376 eV/408.16 nm	0.0282	192 -> 198	0.27320	d ->d, L ->L'
			193 -> 197	0.15634	M ->L', L ->L'
			193 -> 198	0.16985	d ->d, L ->L'
$S_0 \rightarrow S_{11}$	3.0574 eV/405.52nm	0.2304	190 -> 195	0.19632	L ->L', M ->L'
			192 -> 195	0.10693	M ->L', L ->L'
			192 -> 196	0.26153	d ->d, L ->L'
			192 -> 198	0.18911	d ->d, L ->L'
			193 -> 195	0.19007	M ->L', L ->L'
			193 -> 196	0.49953	d ->d, L ->L'
			193 -> 197	0.15983	M ->L', L ->L'
$S_0 \rightarrow S_{12}$	3.0767 eV/402.98 nm	0.0957	190 -> 195	0.51368	L ->L', M ->L'
			192 -> 195	0.10233	M ->L', L ->L'
			192 -> 196	0.20748	d ->d, L ->L'
			193 -> 195	0.10656	L ->L', M ->L'
			193 -> 196	0.27452	d ->d, L ->L'
			193 -> 198	0.25900	d ->d, L ->L'
$S_0 \rightarrow S_{13}$	3.1295 eV/396.18 nm	0.3002	192 -> 197	0.23447	M ->L', L ->L'
			192 -> 198	0.34458	d ->d, L ->L'
			193 -> 195	0.12908	L ->L', M ->L'
			193 -> 196	0.21443	d ->d, L ->L'
			193 -> 197	0.43502	M ->L', L ->L'
			193 -> 198	0.19124	d ->d, L ->L'
$S_0 \rightarrow S_{14}$	3.1834 eV/389.47 nm	0.0005	190 -> 195	0.42016	L ->L', M ->L'
			192 -> 195	0.11688	L ->L', M ->L'
			192 -> 196	0.43253	d ->d, L ->L'
			192 -> 198	0.13864	d ->d, L ->L'
			193 -> 196	0.11101	d ->d, L ->L'
			193 -> 198	0.24588	d ->d, L ->L'
			186 -> 195	0.35474	L ->L', IL

$S_0 \rightarrow S_{15}$	3.2639 eV/379.86 nm	0.0039	186 -> 196	0.10300	$L \rightarrow L', L \rightarrow M$
			187 -> 195	0.55549	$L \rightarrow L', IL$
			187 -> 196	0.14730	$L \rightarrow L', L \rightarrow M$
			188 -> 195	0.12070	$M \rightarrow L', L \rightarrow L'$
$S_0 \rightarrow S_{16}$	3.2838 eV/377.56 nm	0.0002	192 -> 196	0.25695	$d \rightarrow d, L \rightarrow L'$
			192 -> 197	0.34826	$M \rightarrow L', L \rightarrow L'$
			192 -> 198	0.18043	$d \rightarrow d, L \rightarrow L'$
			193 -> 196	0.12217	$d \rightarrow d, L \rightarrow L'$
			193 -> 197	0.12566	$M \rightarrow L', L \rightarrow L'$
			193 -> 198	0.43533	$d \rightarrow d, L \rightarrow L'$
			194 -> 202	0.14367	$d \rightarrow d, L \rightarrow L'$
$S_0 \rightarrow S_{17}$	3.4802 eV/356.26 nm	0.0160	186 -> 195	0.56982	$L \rightarrow L', IL$
			186 -> 196	0.15879	$L \rightarrow L', L \rightarrow M$
			187 -> 195	0.34190	$L \rightarrow L', IL$
$S_0 \rightarrow S_{18}$	3.5488 eV/349.37 nm	0.0175	191 -> 196	0.67037	$d \rightarrow d, L \rightarrow L'$
			194 -> 199	0.11229	$d \rightarrow d, L \rightarrow L'$
$S_0 \rightarrow S_{19}$	3.5939 eV/344.98 nm	0.0076	191 -> 196	0.10083	$d \rightarrow d, L \rightarrow L'$
			194 -> 196	0.11573	$M \rightarrow L', L \rightarrow L'$
			194 -> 199	0.65652	$d \rightarrow d, L \rightarrow L'$
$S_0 \rightarrow S_{20}$	3.6356 eV/341.03 nm	0.0002	190 -> 197	0.12402	$M \rightarrow L', L \rightarrow L'$
			191 -> 197	0.61039	$M \rightarrow L', L \rightarrow L'$
			191 -> 198	0.27527	$M \rightarrow L', L \rightarrow L'$
			188 -> 195	0.38137	$M \rightarrow L', L \rightarrow L'$
			189 -> 195	0.56342	$M \rightarrow L', L \rightarrow L'$

^a Only the electronic transitions with excitation energy lower than 350 nm are presented.

^b Oscillator strength.

^c Only the main configurations are presented.

^d The CI coefficients are in absolute values.

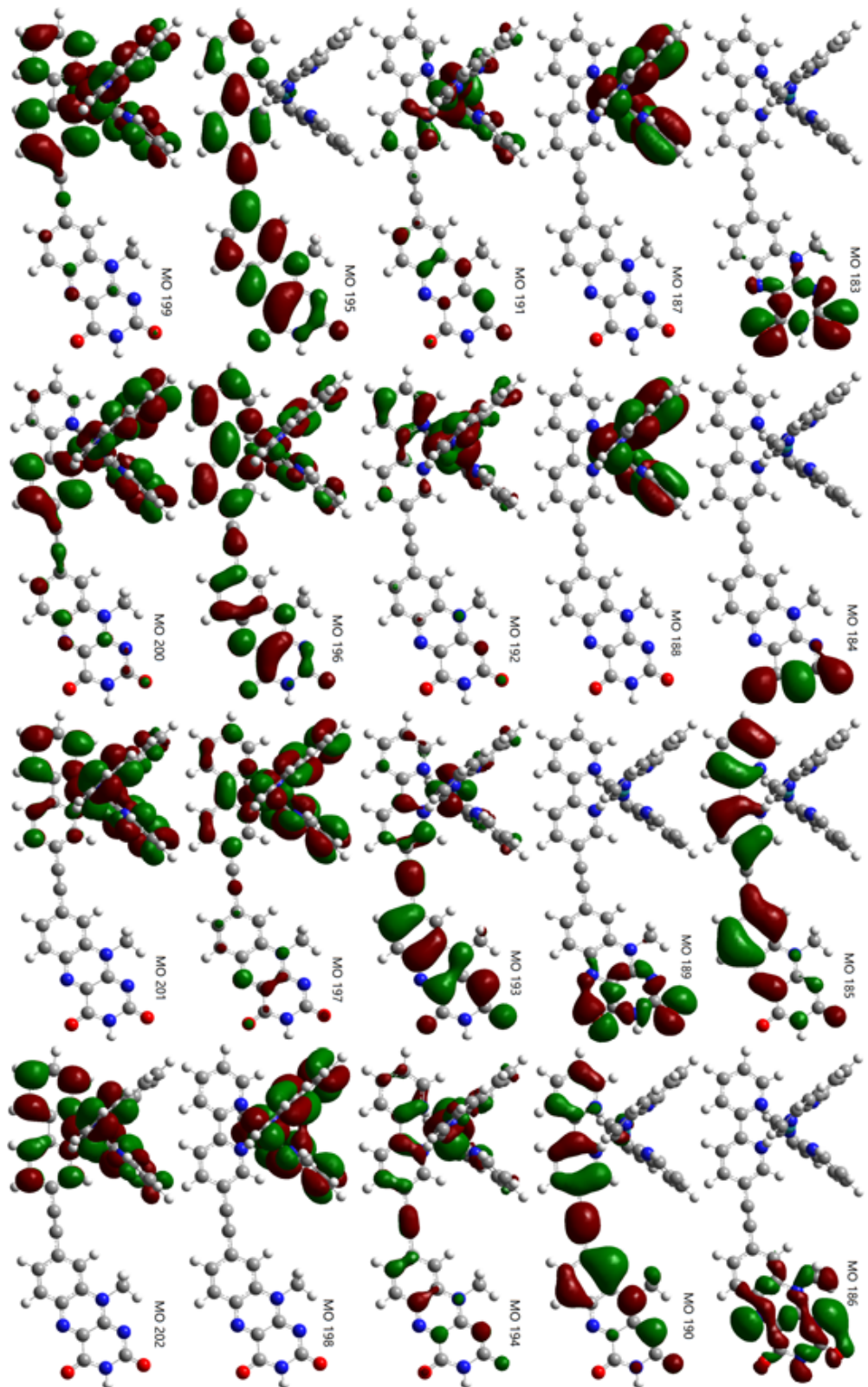


Figure S36. Contour plots of wavefunction of states of Ru-1 involved in absorption in visible light region. The Ru, C, O, N, H and etc are in cyan, gray, red, blue and white, respectively. The isovalue is ± 0.02 a.u.

Table S2. Electronic transitions involved in the excitation of Ru-1 in visible light region (Calculated with TD-PBE0 functional at 6-31g(d,p)//lanl2dz level).

Transitions	Energy ^a	f ^b	Composition ^c	CI ^d	Character
$S_0 \rightarrow S_1$	2.5751 eV/481.47 nm	0.0440	193 ->195	0.12481	M ->L', L ->L'
			193 ->196	0.10161	M ->L', L ->L'
			194 ->195	0.59682	M ->L', L ->L'
			194 ->196	0.27376	M ->L', d ->d
			194 ->197	0.17591	d ->d, L ->L'
$S_0 \rightarrow S_2$	2.7630 eV/448.73 nm	0.2900	191 ->195	0.16871	M ->L', L ->L'
			191 ->196	0.11213	M ->L', d ->d
			192 ->195	0.39206	M ->L', L ->L'
			192 ->196	0.22644	M ->L', d ->d
			192 ->197	0.11593	d ->d, L ->L'
			193 ->195	0.45184	M ->L', L ->L'
			194 ->195	0.11394	M ->L', L ->L'
$S_0 \rightarrow S_3$	2.8139 eV/440.61 nm	0.6939	191 ->195	0.47597	M ->L', L ->L'
			191 ->196	0.15638	M ->L', d ->d
			192 ->195	0.19668	M ->L', L ->L'
			193 ->195	0.40023	M ->L', L ->L'
			194 ->195	0.12124	M ->L', L ->L'
$S_0 \rightarrow S_4$	2.8663 eV/432.56 nm	0.1477	191 ->195	0.36089	M ->L', L ->L'
			191 ->196	0.18981	M ->L', d ->d
			192 ->195	0.43342	M ->L', L ->L'
			192 ->196	0.15896	M ->L', d ->d
			193 ->195	0.26656	M ->L', L ->L'
			194 ->198	0.15310	d ->d, L ->L'
$S_0 \rightarrow S_5$	2.9091 eV/426.19 nm	0.0077	193 ->198	0.20172	d ->d, L ->L'
			194 ->196	0.12043	M ->L', d ->d
			194 ->197	0.19071	d ->d, L ->L'
			194 ->198	0.60434	d ->d, L ->L'

S₀→S₆	2.9184 eV/424.83 nm	0.0015	193 ->197	0.18801	d ->d, L ->L'
			194 ->196	0.28724	M ->L', d ->d
			194 ->197	0.55047	d ->d, L ->L'
			194 ->198	0.21360	d ->d, L ->L'
S₀→S₇	3.1097 eV/398.70 nm	0.0064	191 ->197	0.19874	d ->d, L ->L'
			191 ->198	0.36644	d ->d, L ->L'
			192 ->196	0.17958	M ->L', d ->d
			192 ->197	0.32808	d ->d, L ->L'
			192 ->198	0.36927	d ->d, L ->L'
			193 ->197	0.14945	d ->d, L ->L'
S₀→S₈	3.1475 eV/393.92 nm	0.0001	191 ->196	0.23222	M ->L', d ->d
			191 ->197	0.42851	d ->d, L ->L'
			191 ->198	0.24089	d ->d, L ->L'
			192 ->196	0.18569	M ->L', d ->d
			192 ->197	0.32373	d ->d, L ->L'
			192 ->198	0.18161	d ->d, L ->L'
			193 ->198	0.13200	d ->d, L ->L'
S₀→S₉	3.2120 eV/386.00 nm	0.0965	190 ->195	0.11050	L ->L',IL
			191 ->196	0.18315	M ->L', d ->d
			191 ->197	0.25897	d ->d, L ->L'
			191 ->198	0.32700	d ->d, L ->L'
			192 ->196	0.17022	M ->L', d ->d
			192 ->197	0.29934	d ->d, L ->L'
			192 ->198	0.28077	d ->d, L ->L'
			193 ->197	0.17154	d ->d, L ->L'
			194 ->196	0.15442	M ->L', d ->d
S₀→S₁₀	3.2406 eV/382.59 nm	0.5325	190 ->195	0.48474	L ->L',IL
			192 ->197	0.14092	d ->d, L ->L'
			192 ->198	0.17406	d ->d, L ->L'

			193 ->196	0.14945	M ->L', L ->L'
			194 ->195	0.20222	M ->L', L ->L'
			194 ->196	0.27933	M ->L', d ->d
			194 ->197	0.15120	d ->d, L ->L'
S₀→S₁₁	3.2667 eV/379.54nm	0.0107	186 ->195	0.42335	L ->L', IL
			186 ->196	0.17312	L ->L', L ->M
			189 ->195	0.45301	L ->L', IL
			189 ->196	0.17305	L ->L', L ->M
S₀→S₁₂	3.2684 eV/379.34 nm	0.1952	189 ->195	0.10257	L ->L', IL
			190 ->195	0.41006	L ->L', IL
			193 ->195	0.13598	M ->L', L ->L'
			194 ->195	0.22305	M ->L', L ->L'
			194 ->196	0.38800	M ->L', d ->d
			194 ->197	0.18928	d ->d, L ->L'
			194 ->199	0.12192	d ->d, L ->L'
S₀→S₁₃	3.3633 eV/368.64 nm	0.1035	190 ->195	0.18871	L ->L', IL
			191 ->195	0.12335	M ->L', L ->L'
			191 ->196	0.21198	M ->L', d ->d
			191 ->197	0.11682	d ->d, L ->L'
			191 ->198	0.32334	d ->d, L ->L'
			192 ->195	0.11447	M ->L', L ->L'
			192 ->196	0.20716	M ->L', d ->d
			192 ->198	0.37684	d ->d, L ->L'
			193 ->198	0.20867	d ->d, L ->L'
S₀→S₁₄	3.3966 eV/365.03 nm	0.0001	183 ->195	0.11495	L ->L', IL
			186 ->195	0.46278	L ->L', IL
			186 ->196	0.18174	L ->L', L ->M
			189 ->195	0.42830	L ->L', IL
			189 ->196	0.15435	L ->L', L ->M

S₀→S₁₅	3.4374 eV/360.69 nm	0.0020	191 ->195	0.19724	M ->L', L ->L'
			191 ->196	0.27913	M ->L', d ->d
			191 ->197	0.14622	d ->d, L ->L'
			192 ->195	0.25197	M ->L', L ->L'
			192 ->196	0.33930	M ->L', d ->d
			192 ->197	0.18365	d ->d, L ->L'
			192 ->199	0.11480	d ->d, L ->L'
			193 ->196	0.27361	M ->L', L ->L'
			193 ->197	0.12209	d ->d, L ->L'
S₀→S₁₆	3.5442 eV/349.83 nm	0.0144	191 ->195	0.16894	M ->L', L ->L'
			191 ->196	0.32617	M ->L', d ->d
			191 ->197	0.28705	d ->d, L ->L'
			191 ->198	0.13086	d ->d, L ->L'
			192 ->195	0.14989	M ->L', L ->L'
			192 ->196	0.31729	M ->L', d ->d
			192 ->197	0.26005	d ->d, L ->L'
			192 ->198	0.13181	d ->d, L ->L'
			194 ->202	0.12556	d ->d, L ->L'
S₀→S₁₇	3.6026 eV/344.16 nm	0.0190	190 ->195	0.13922	L ->L', IL
			191 ->196	0.25081	M ->L', d ->d
			192 ->196	0.18527	M ->L', d ->d
			193 ->196	0.56473	M ->L', L ->L'
			193 ->197	0.10630	d ->d, L ->L'
			194 ->196	0.15392	M ->L', d ->d
S₀→S₁₈	3.7232 eV/333.01 nm	0.0028	190 ->197	0.13392	L ->L', L ->M
			191 ->197	0.16924	d ->d, L ->L'
			192 ->197	0.13981	d ->d, L ->L'
			193 ->197	0.52491	d ->d, L ->L'
			193 ->198	0.25461	d ->d, L ->L'

194 ->197 0.18952 d ->d, L ->L'

^a Only the electronic transitions with excitation energy lower than 350 nm are presented.

^b Oscillator strength.

^c Only the main configurations are presented.

^d The CI coefficients are in absolute values.

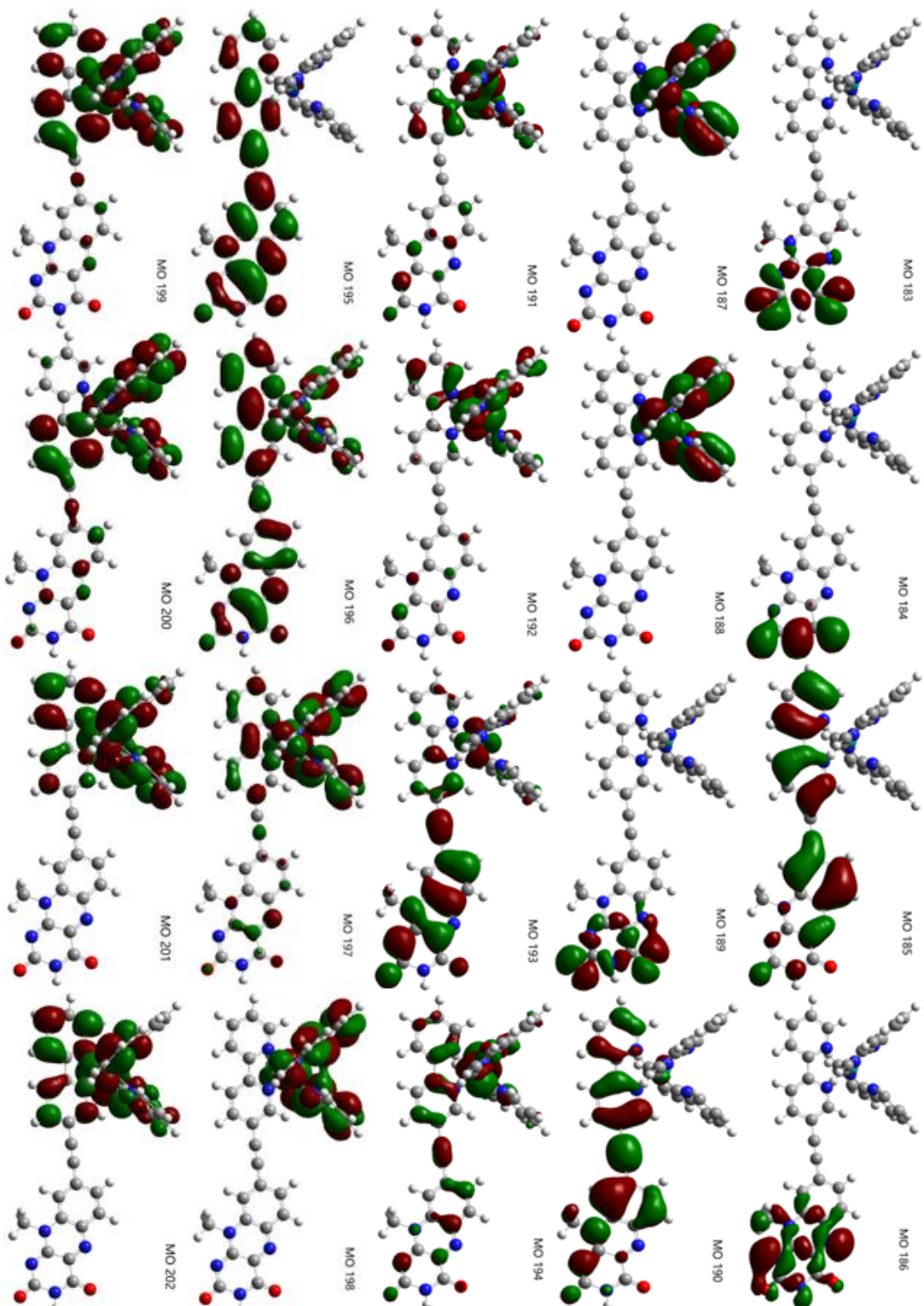
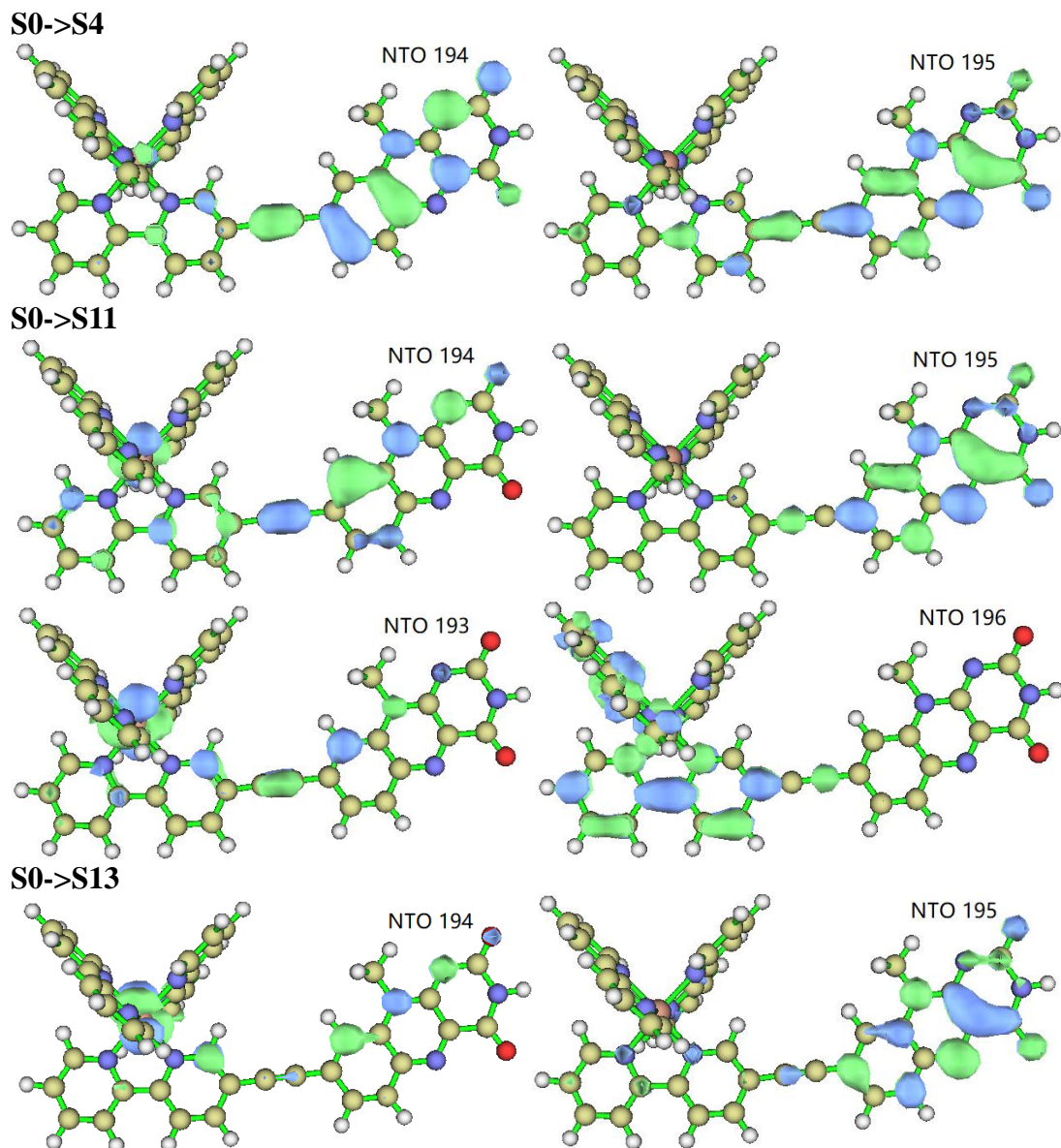


Figure S37. Contour plots of wavefunction of states of Ru-1 involved in absorption in visible light region calculated at TD-PBE0/6-31g(d,p)//LanL2dz level. The Ru, C, O, N, H and etc are in cyan, gray, red, blue and white, respectively. The isovalue is ± 0.02 a.u.

Table S3. NTO analysis of selected transitions of Ru-1 in visible light region (Calculated with TD-B3LYP functional at 6-31g(d)//lanl2dz level).

Transitions	NTO pairs contribute mainly to the transition	Contribution of the NTO pair (%)	Character	Contribution of Ru states (%)
S0->S4	NTO 194 – NTO 195	94.62%	IL、 M ->L	5.56%
S0->S11	NTO 194 – NTO 195	61.81%	M ->L、 IL	51.10%
	NTO 193 – NTO 196	29.03%	M ->L、 L ->L'	35.35%
S0->S13	NTO 194 – NTO 195	50.54%	M ->L、 L ->L'	62.81%
	NTO 193 – NTO 196	29.07%	M ->L、 L ->L'	24.90%
	NTO 192 – NTO 197	14.25%	M ->L	76.81%



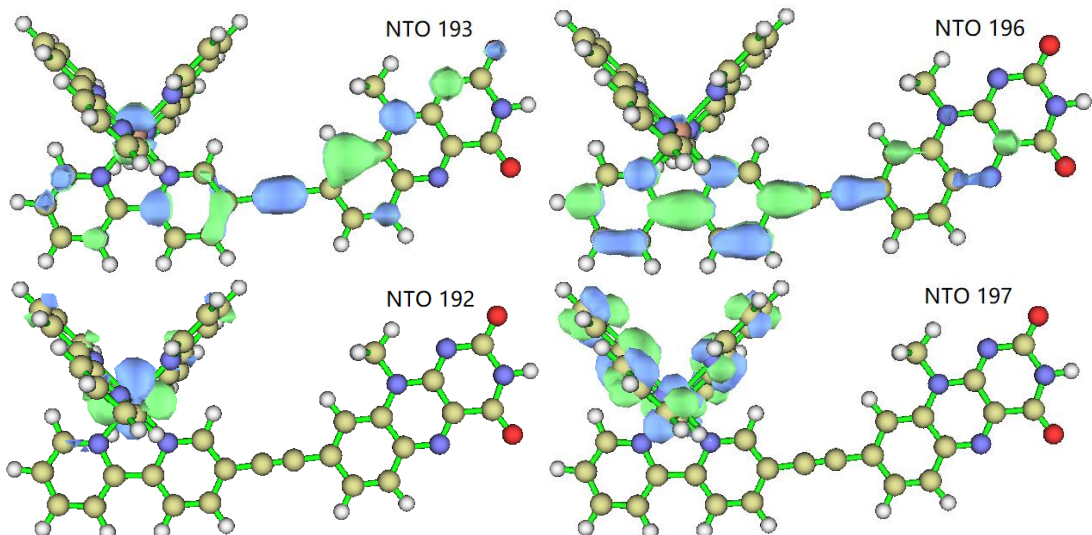
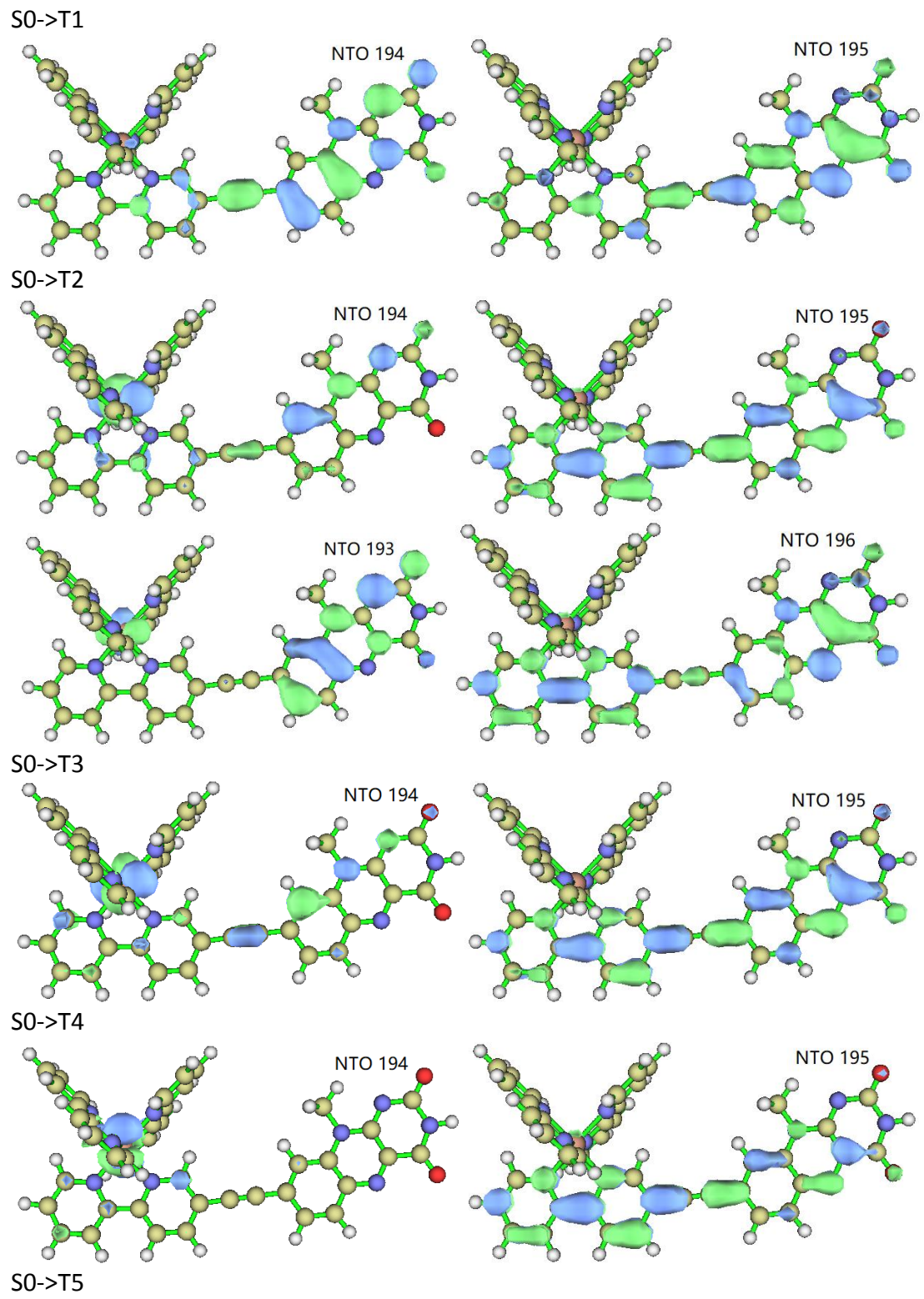


Figure S38. Contour plots of NTO pairs contributed mainly to absorption of Ru-1. The Ru, C, O, N, H and etc are in bronze, dark yellow, red, blue and white, respectively. The isovalue is ± 0.02 a.u.

Table S3. NTO analysis of low lying $S_0 \rightarrow T_n$ transitions of Ru-1 (Calculated with TD-B3LYP functional at 6-31g(d)//lanl2dz level).

Transitions	NTO pairs contribute mainly to the transition	Contribution of the NTO pair (%)	Character	Contribution of Ru states (%)
$S_0 \rightarrow T_1$	NTO 194 – NTO 195	90.13%	IL	2.37%
$S_0 \rightarrow T_2$	NTO 194 – NTO 195	75.33%	M \rightarrow L, IL	54.03%
	NTO 193 – NTO 196	14.95%	M \rightarrow L, L \rightarrow L'	20.96%
$S_0 \rightarrow T_3$	NTO 194 – NTO 195	81.88%	M \rightarrow L, IL	58.58%
$S_0 \rightarrow T_4$	NTO 194 – NTO 195	89.60%	M \rightarrow L	76.25%
$S_0 \rightarrow T_5$	NTO 194 – NTO 195	89.90%	M \rightarrow L	76.53%



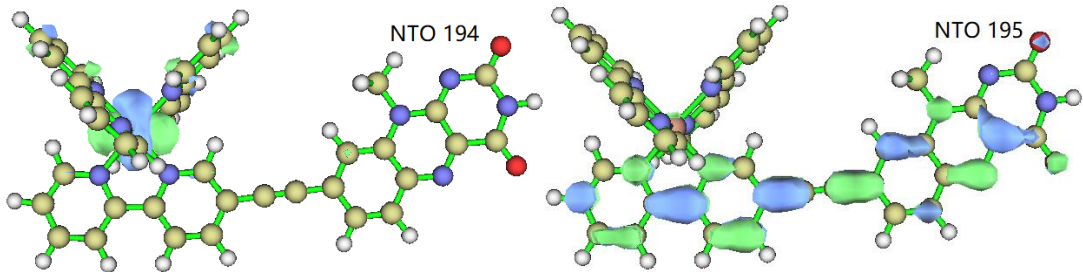


Figure S39. Contour plots of NTO pairs contributed mainly to low lying $S_0 \rightarrow T_n$ transitions of Ru-1. The Ru, C, O, N, H and etc are in bronze, dark yellow, red, blue and white, respectively. The isovalue is ± 0.02 a.u.